

LLNL Modeling Calculations in Support of the NMD EOS Program: FY01 3Q Report

M. Gerassimenko

July 1, 2001

U.S. Department of Energy

Lawrence
Livermore
National
Laboratory

DISCLAIMER

This document was prepared as an account of work sponsored by an agency of the United States Government. Neither the United States Government nor the University of California nor any of their employees, makes any warranty, express or implied, or assumes any legal liability or responsibility for the accuracy, completeness, or usefulness of any information, apparatus, product, or process disclosed, or represents that its use would not infringe privately owned rights. Reference herein to any specific commercial product, process, or service by trade name, trademark, manufacturer, or otherwise, does not necessarily constitute or imply its endorsement, recommendation, or favoring by the United States Government or the University of California. The views and opinions of authors expressed herein do not necessarily state or reflect those of the United States Government or the University of California, and shall not be used for advertising or product endorsement purposes.

This work was performed under the auspices of the U. S. Department of Energy by the University of California, Lawrence Livermore National Laboratory under Contract No. W-7405-Eng-48.

This report has been reproduced
directly from the best available copy.

Available to DOE and DOE contractors from the
Office of Scientific and Technical Information
P.O. Box 62, Oak Ridge, TN 37831
Prices available from (423) 576-8401
<http://apollo.osti.gov/bridge/>

Available to the public from the
National Technical Information Service
U.S. Department of Commerce
5285 Port Royal Rd.,
Springfield, VA 22161
<http://www.ntis.gov/>

OR

Lawrence Livermore National Laboratory
Technical Information Department's Digital Library
<http://www.llnl.gov/tid/Library.html>

Introduction

A program to examine equation-of-state (EOS) issues of interest to the National Missile Defense (NMD) program has been underway for a couple of years. There are current plans to conduct experiments at Sandia National Laboratory in Albuquerque. The initial experiments will be two-dimensional: a thin flyer will normally impact a target at two nominal velocities 6 km/s and 11 km/s. A witness plate is placed parallel to the target, separated from it by a 75 mm gap. Several channels of VISAR measure the particle velocity at different locations at the rear of the witness plate. A schematic of the experimental configuration is shown in Figure 1.

At a kick-off meeting in March 2001, the initial computational task for all three laboratories (SNLA, LANL, and LLNL) was to calculate the witness plate particle velocity profiles produced by the two contemplated projectile sizes at both projectile velocities. This report documents these calculations as well as further calculations prompted by the initial results.

First Series of Modeling Calculations

Calculations setup

Modeling calculations are done with the CALE code, which is a 2-D axisymmetric hydrodynamics code with arbitrary Lagrange Eulerian capabilities. In these calculations, there is an axis of rotational symmetry located at zero in the radial direction. Physically, zones are hoops whose axis is this rotational symmetry axis. Many figures in this report are cross sections with the rotational symmetry axis running left to right. The radial coordinate (r) is up down, the axial coordinate z is left right. The calculation setup for a 12.7 mm diameter projectile is shown in Figure 2. The rotational symmetry axis is at $r=0$ and zoning is indicated in the upper half. The projectile, target and witness plate appear as rectangles, but this is a cross section so they are physically thin cylinders. Zoning is difficult to see for the projectile, target and witness plate, it is better visible in the close-ups shown in Figures 3 and 4. The calculational setup and close up for a 17 mm diameter projectile are shown in Figures 5 and 6. Tracer points that move with the material are located at the rear of the witness plate on axis and at 2 mm intervals radially.

Standard zoning is 140x113 zones along the axis and radius, respectively. This amounts to 9 zones across the thickness of the projectile 10 zones across the thickness of the target and the witness plate, the target and the witness plate as well as 100 zones across the 75 mm gap between the target and the witness plate. Radially zoning is close to uniform with 9 zones across the 6.35 mm radius projectile and 12 across the 8.5 mm radius one.

The background material is vacuum with a density of 10^{-6} g/cm³. The projectile EOS is a Gruneisen one with coefficients determined for Ti6Al4V which is the titanium alloy the projectile is made of. The target EOS is a tabular one, referred to as LEOS at LLNL, which treats all phases of materials. The EOS treats the heterogeneous silicate phenolic as a homogeneous material. The witness plate EOS is a polynomial one with coefficients determined for the 6061-T6 aluminum alloy. All material constitutive models are elastic plastic. Material failure (zero strength) takes place when the tensile strength is exceeded in tension or when the accumulated effective plastic strain exceeds the maximum specified in the constitutive model. Material parameters are listed in Table 1.

Table 1
Material Parameters

Projectile:	Gruneisen EOS for Ti6Al4V alloy density = 4.419 g/cm ³ coefficients $c=0.513$, $S1=1.028$, $S2=0$, $S3=0$, $G0=1.23$, $A=0.17$ modulus = 419 kbars, yield strength = 13.2 kbars maximum effective plastic strain = 2 tensile strength = 25 kbars
Target:	LEOS for silicate phenolic (LEOS 7020) density = 1.644 g/cm ³ modulus = 232 kbars, yield strength = 2 kbars no effective plastic strain based failure tensile strength = 2 kbars
Witness plate:	polynomial EOS for 6061 T6 aluminum alloy density = 2.703 g/cm ³ coefficients $A0=0$, $A1=0.742179$, $A2=0.604876$, $A3=0.187029$, $B0=1.97$, $B1=0.48$, $B3=0$ modulus = 276 kbars, yield strength = 2.9 kbars maximum effective plastic strain = 0.5 tensile strength = 12 kbars

Results of the Calculations

Results of the modeling calculations for a 12.7 mm diameter projectile at 6 km/s initial velocity are shown in Figures 7 and 8. Figure 7 is a materials map at the end of the calculation with zoning indicated above the symmetry axis. The particle velocity profiles, at the rear of the witness plate, on axis and 2, 4, and 6 mm away are shown in Figure 8. Analogous results for a 17 mm diameter projectile are shown in Figures 9 and 10. Analogous results for an initial projectile velocity of 11 km/s are shown in Figures 11 through 14.

Second Series of Modeling Calculations

To increase the meaningful length of the particle velocity record, we back the witness plate with a 10 mm thick LiF window. It is well known that the shock impedance of LiF is nearly identical to that of aluminum. We also restrict our attention to 17 mm diameter projectiles. Finally, we examine the effect of target strength and zoning on the calculated particle velocity profiles.

The model setup and close-ups with zoning are shown in Figures 15 through 17. Results for 6 km/s initial projectile velocity are shown in Figures 18 and 19, and Figures 20 and 21 for 11 km/s initial projectile velocity.

We investigate the effect of target strength by running calculations in which the yield strength of the target is doubled and halved. The results are shown in Figures 22 through 25 for 6 km/s initial projectile velocity. The calculated profiles, near axis, are shown in Figure 26. It is clear that the target yield strength strongly affects the calculated particle velocity profiles, both in amplitude and timing. Analogous results for an initial projectile velocity of 11 km/s are shown in Figures 27 through 31. At this higher velocity, the target strength has an even more dramatic effect on the calculated particle velocity peak amplitude.

Finally, we examine the effect of resolution by increasing zoning from 150x113 in the standard calculations with LiF backing to 240x225 zones. We keep the same number of zones across the thickness of the projectile target, witness plate and backing, but increase it by a factor of two across the gap and in the radial direction.

The model setup and close-ups with zoning are shown in Figures 32 through 34. Results for 6 km/s initial projectile velocity are shown in Figures 35 and 36. Analogous results for 11 km/s initial projectile velocity are shown in Figures 37 and 38. Comparison of the calculated particle velocity profiles with those obtained with standard zoning show little dependence on zoning. Direct comparisons of the particle velocity profiles on axis are shown in Figures 39 and 40.

Experimental Approach - I

- “Simple” 2-D/1 experiments
 - 0.8 mm Ti plates at 6 and 11 km/s striking SiPh target; 12.7 and 17 mm diameter
 - SiPh samples 4 mm thick
 - Photographs of debris cloud
 - Multiple visar recording on witness plate
 - Witness Plate 4 mm thick
 - Stand off distance 75 mm

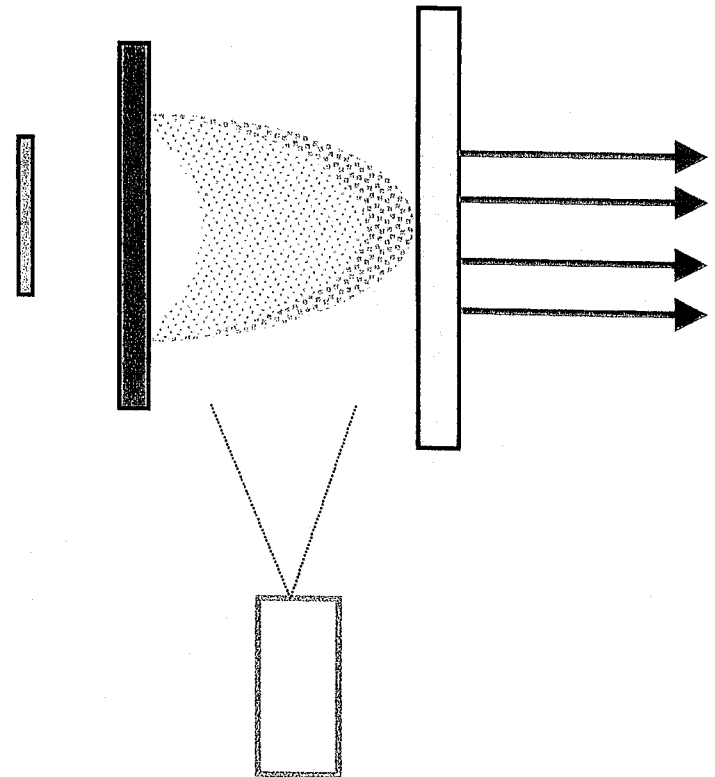
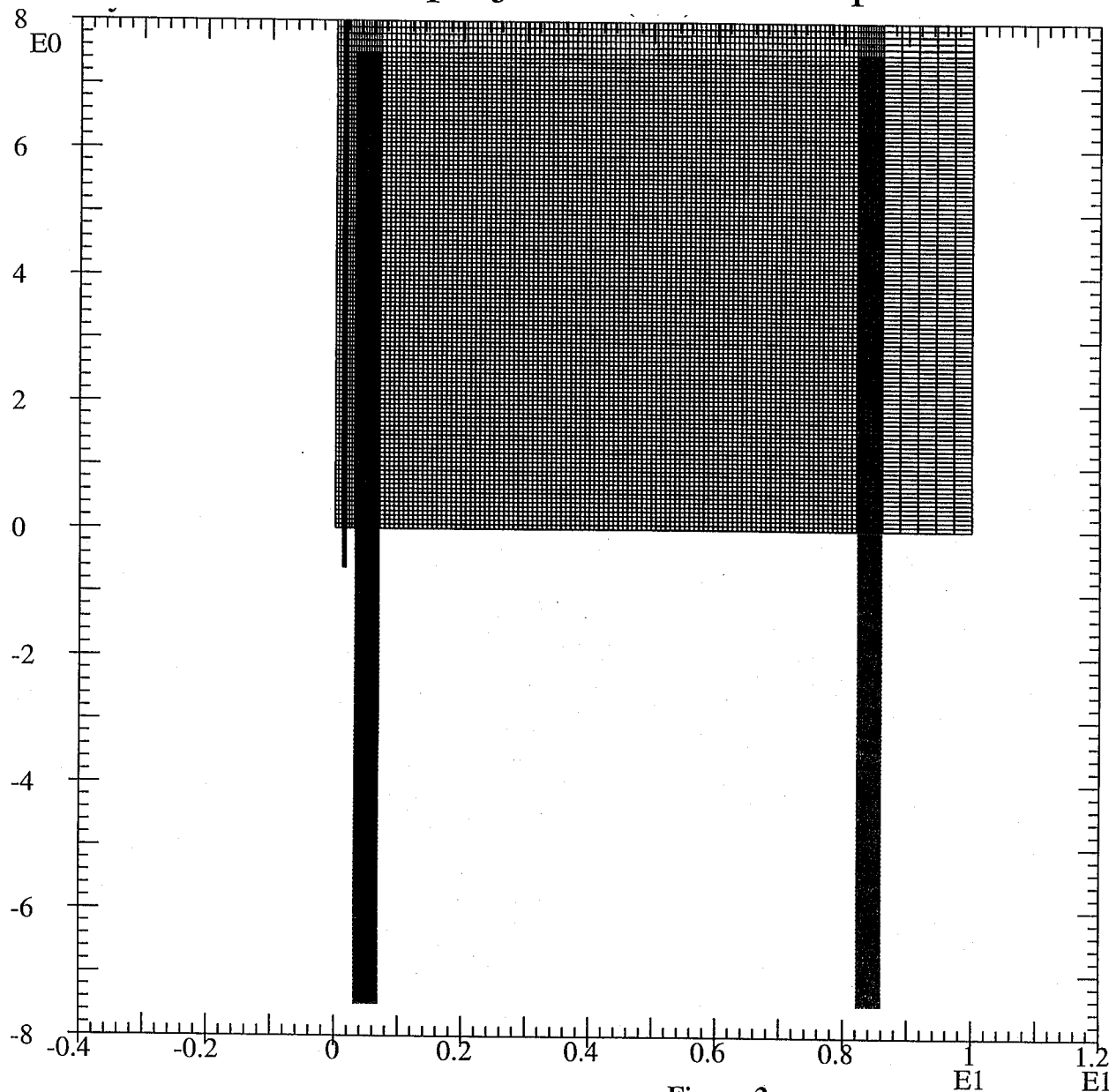


Figure 1

First series NMD EOS experiments modeling calculations

12.7mm diameter projectile: materials plot and zoning



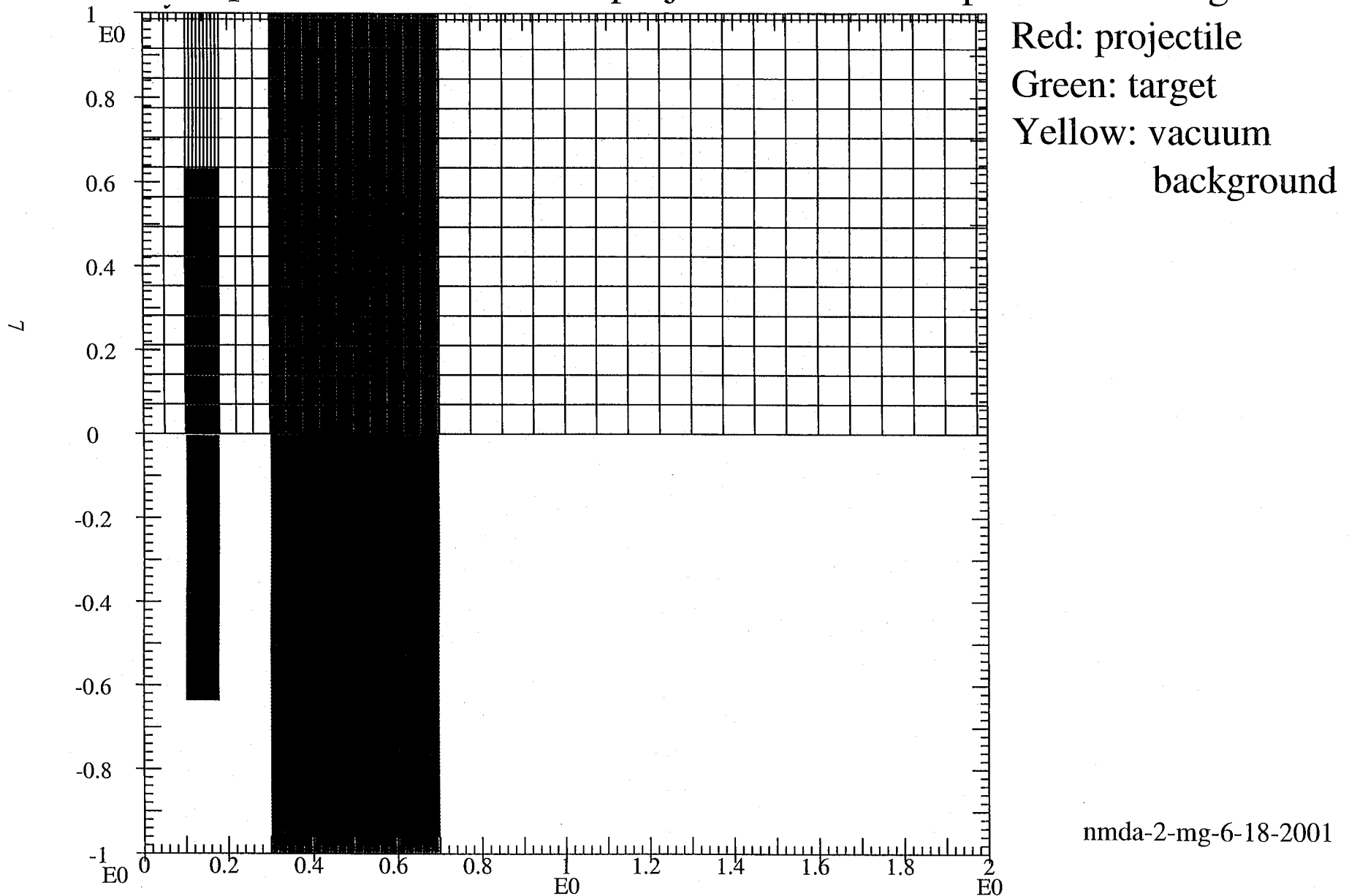
Red: projectile
Green: target
Blue: witness plate
Yellow: vacuum
background

Figure 2

nmda-1-mg-6-18-2001

First series NMD EOS experiments modeling calculations

Closeup of 12.7mm diameter projectile: materials plot and zoning



nmda-2-mg-6-18-2001

Figure 3

First series NMD EOS experiments modeling calculations



Closeup of witness plate and gap: materials plot and zoning

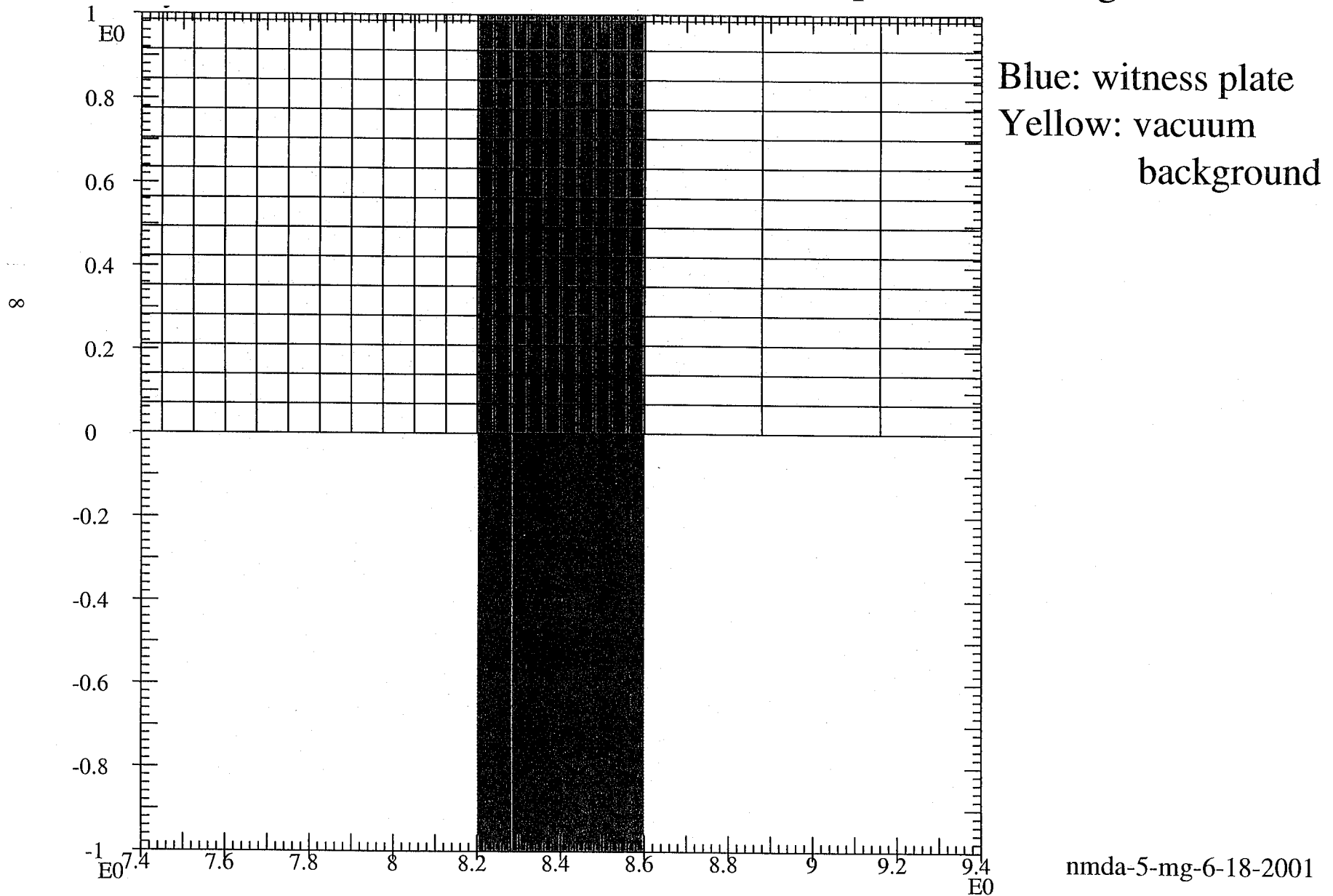


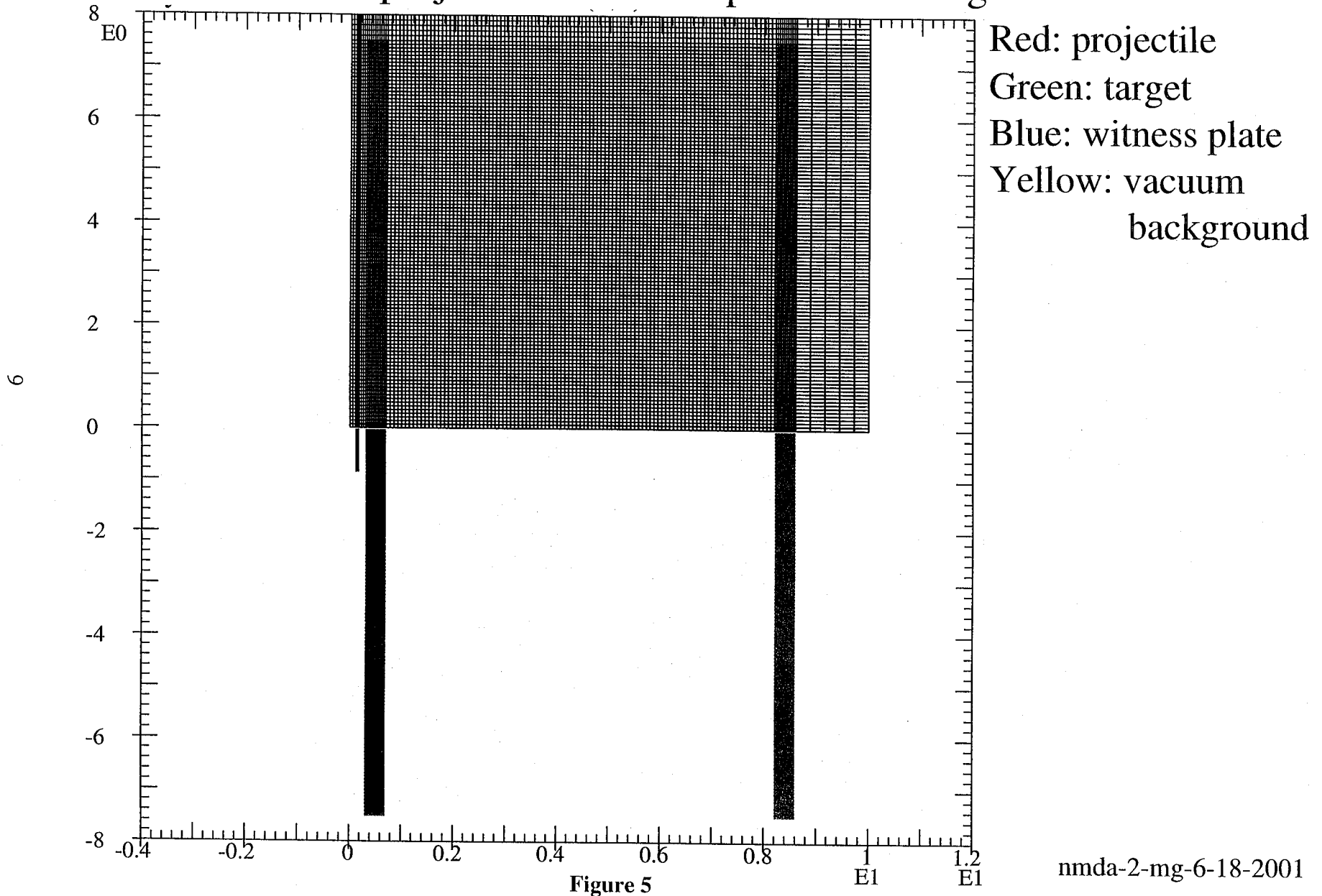
Figure 4

nmda-5-mg-6-18-2001

First series NMD EOS experiments modeling calculations



17mm diameter projectile: materials plot and zoning



First series NMD EOS experiments modeling calculations



Closeup of 17mm diameter projectile: materials plot and zoning

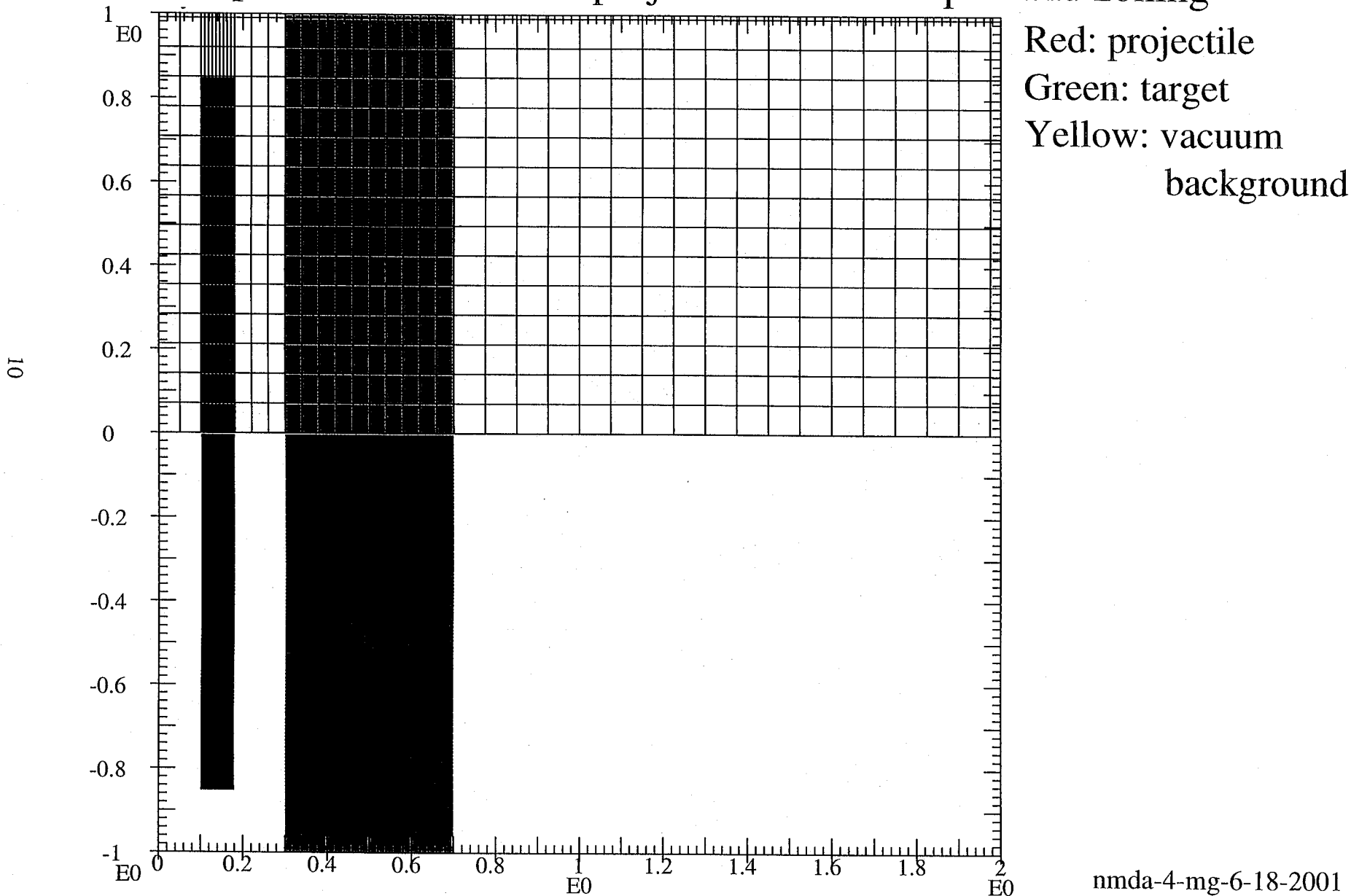


Figure 6

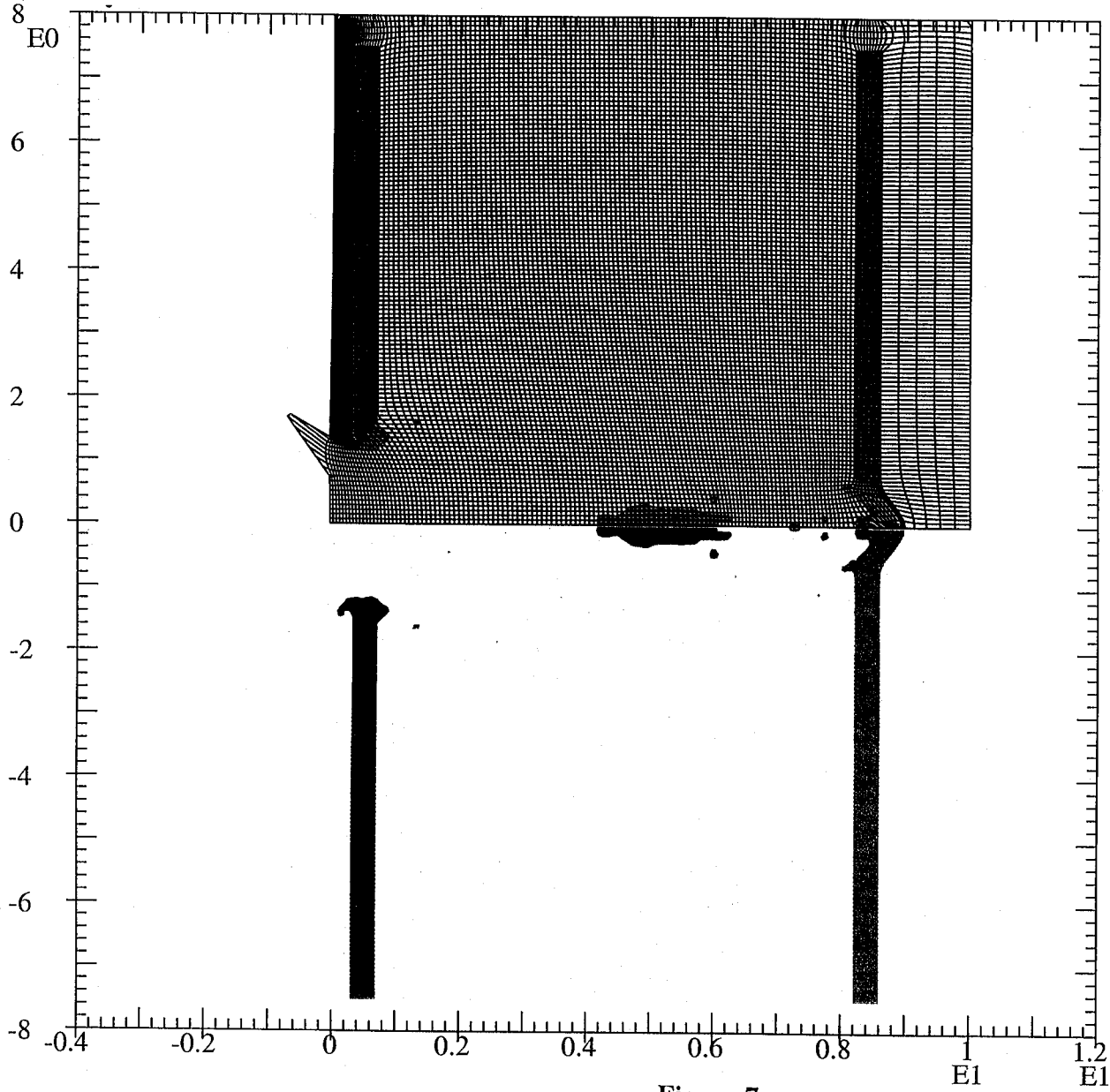
nmda-4-mg-6-18-2001

First series NMD EOS experiments modeling calculations



12.7mm diameter projectile at 6km/s:t=20μs materials plot and zoning

11



Red: projectile
Green: target
Blue: witness plate
Yellow: vacuum
background

Figure 7

nmda--7-mg-6-18-2001

First series NMD EOS experiments modeling calculations



12.7mm diameter projectile at 6km/s

Particle velocities at rear of witness plate on axis and 2,4 and 6mm away

12

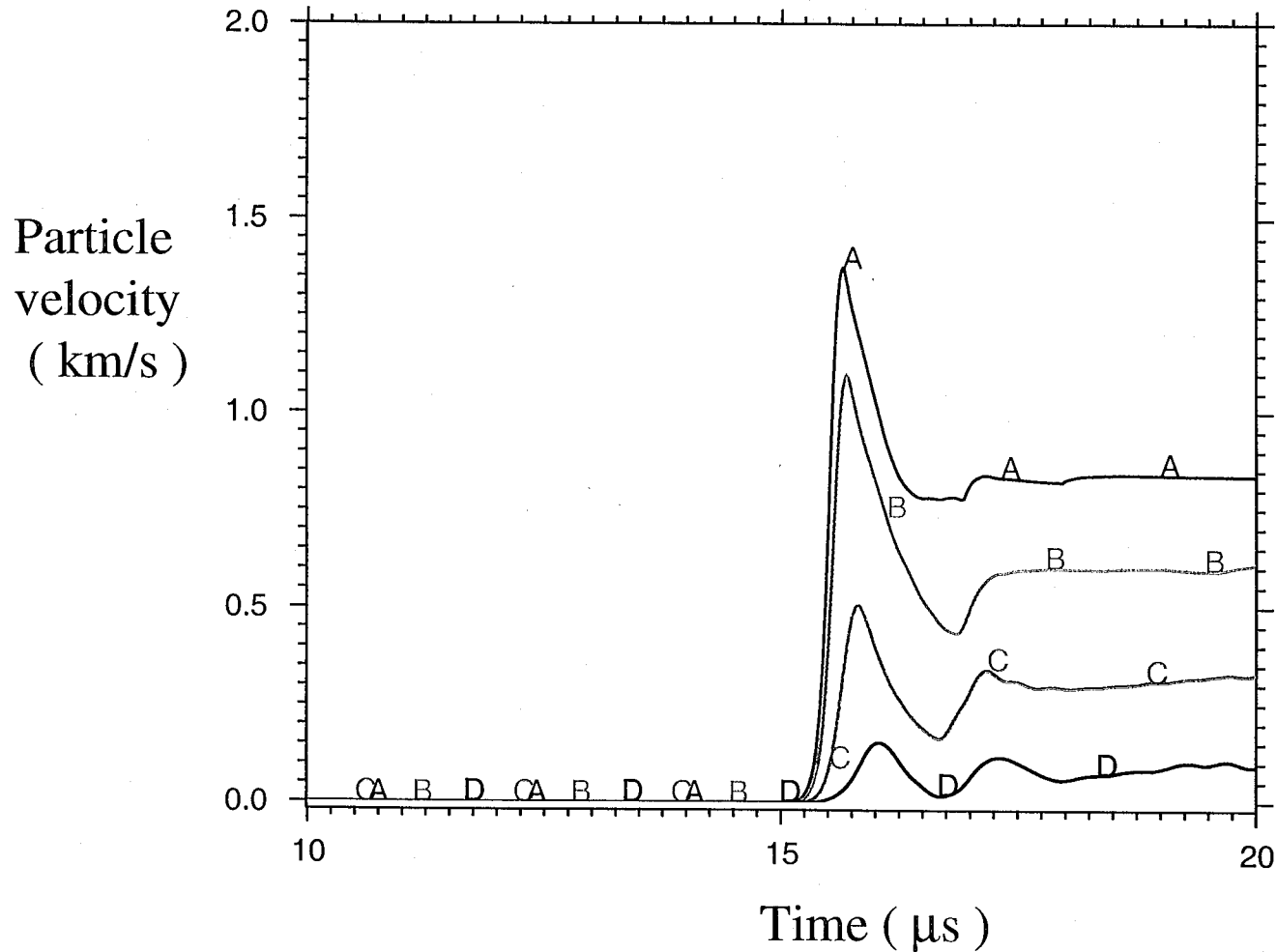
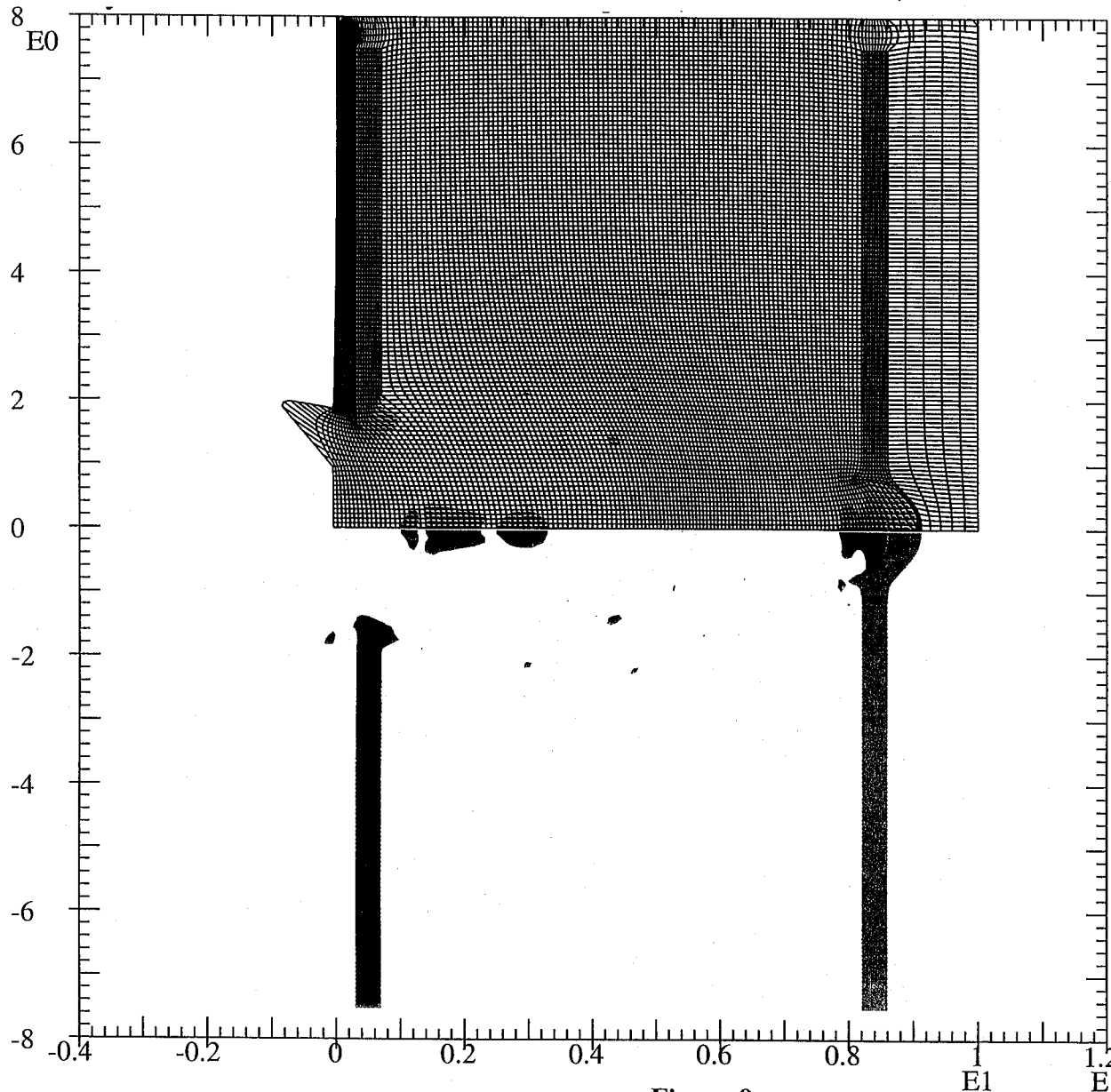


Figure 8

First series NMD EOS experiments modeling calculations



17mm diameter projectile at 6km/s:t=20μs materials plot and zoning



Red: projectile
Green: target
Blue: witness plate
Yellow: vacuum
background

13

Figure 9

nmda--6-mg-6-18-2001

First series NMD EOS experiments modeling calculations



17mm diameter projectile at 6km/s

Particle velocities at rear of witness plate on axis and 2,4 and 6mm away

14

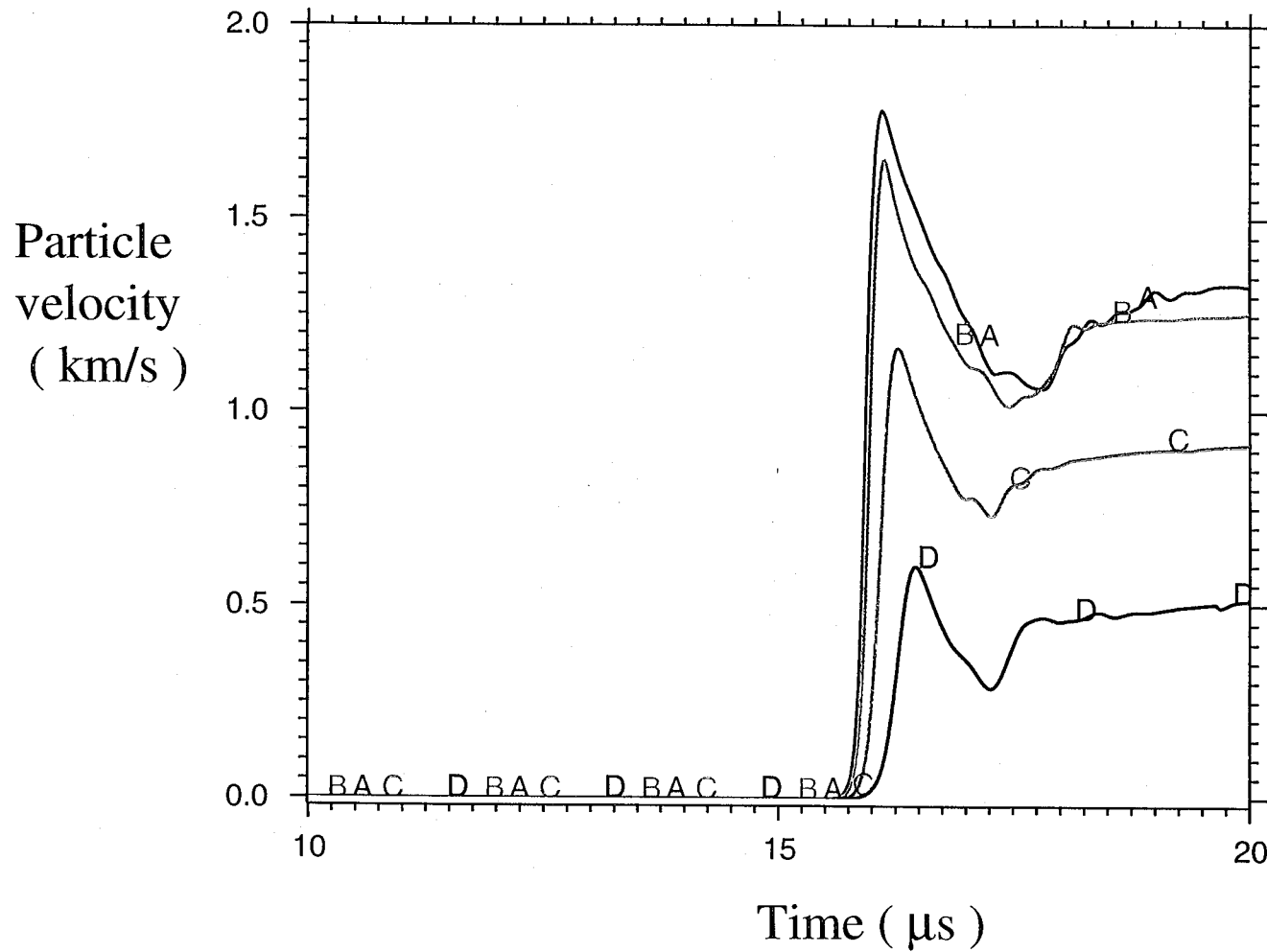


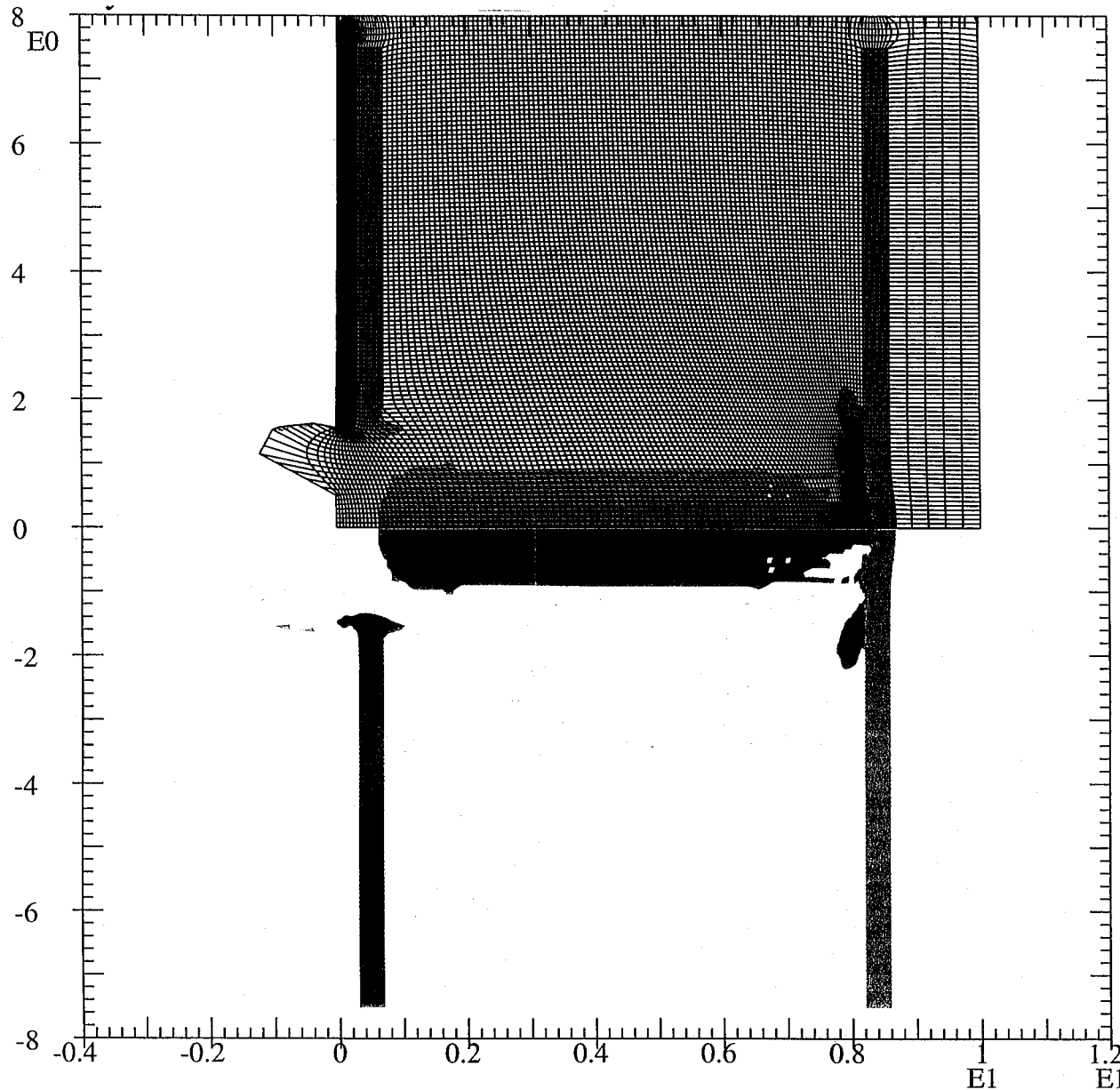
Figure 10

First series NMD EOS experiments modeling calculations



12.7mm diameter projectile at 11km/s:t=12μs materials plot and zoning

15



Red: projectile
Green: target
Blue: witness plate
Yellow: vacuum
background

nmda--8-mg-6-18-2001

Figure 11

First series NMD EOS experiments modeling calculations



12.7mm diameter projectile at 11km/s

Particle velocities at rear of witness plate on axis and 2,4 and 6mm away

16

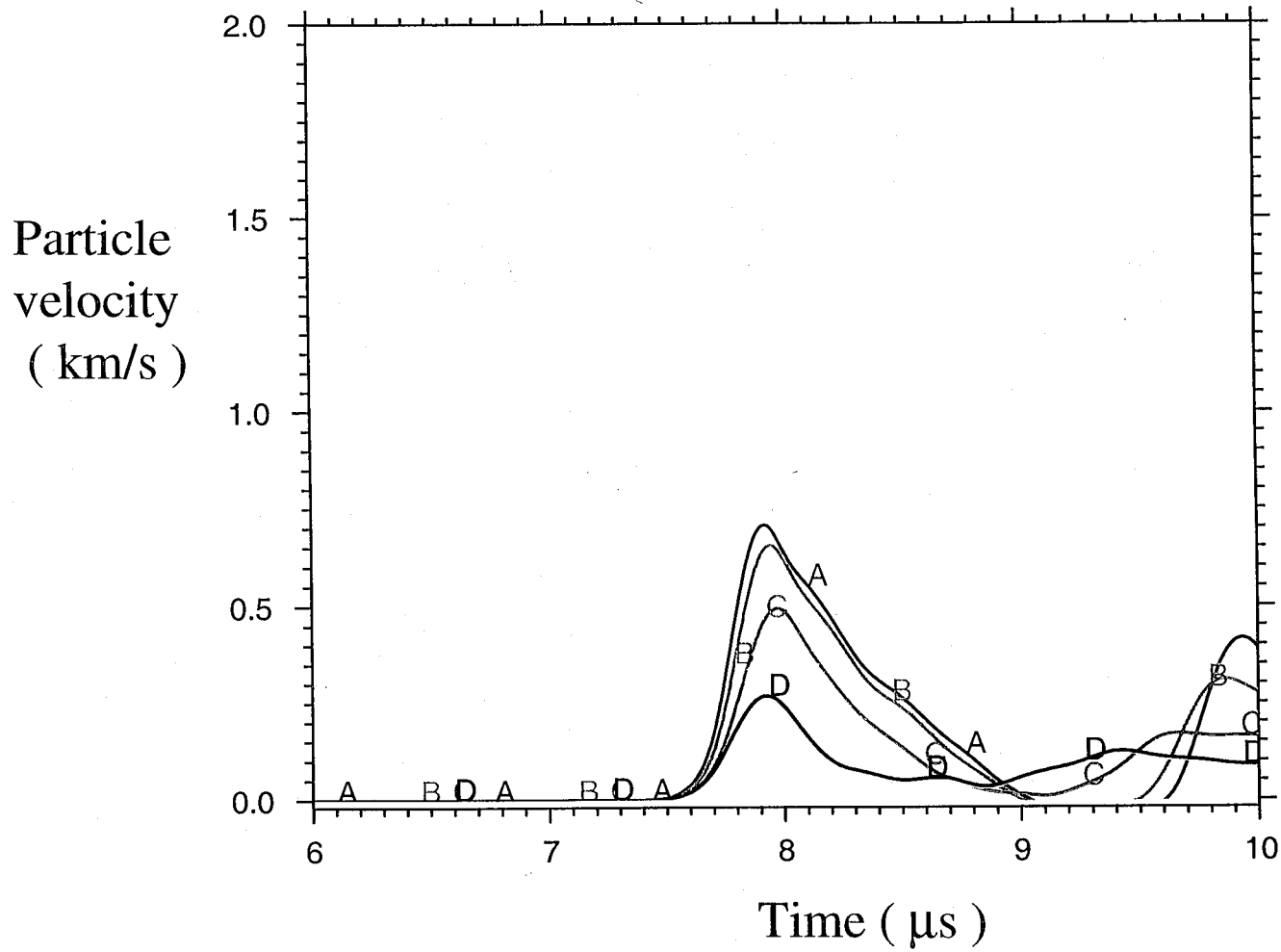


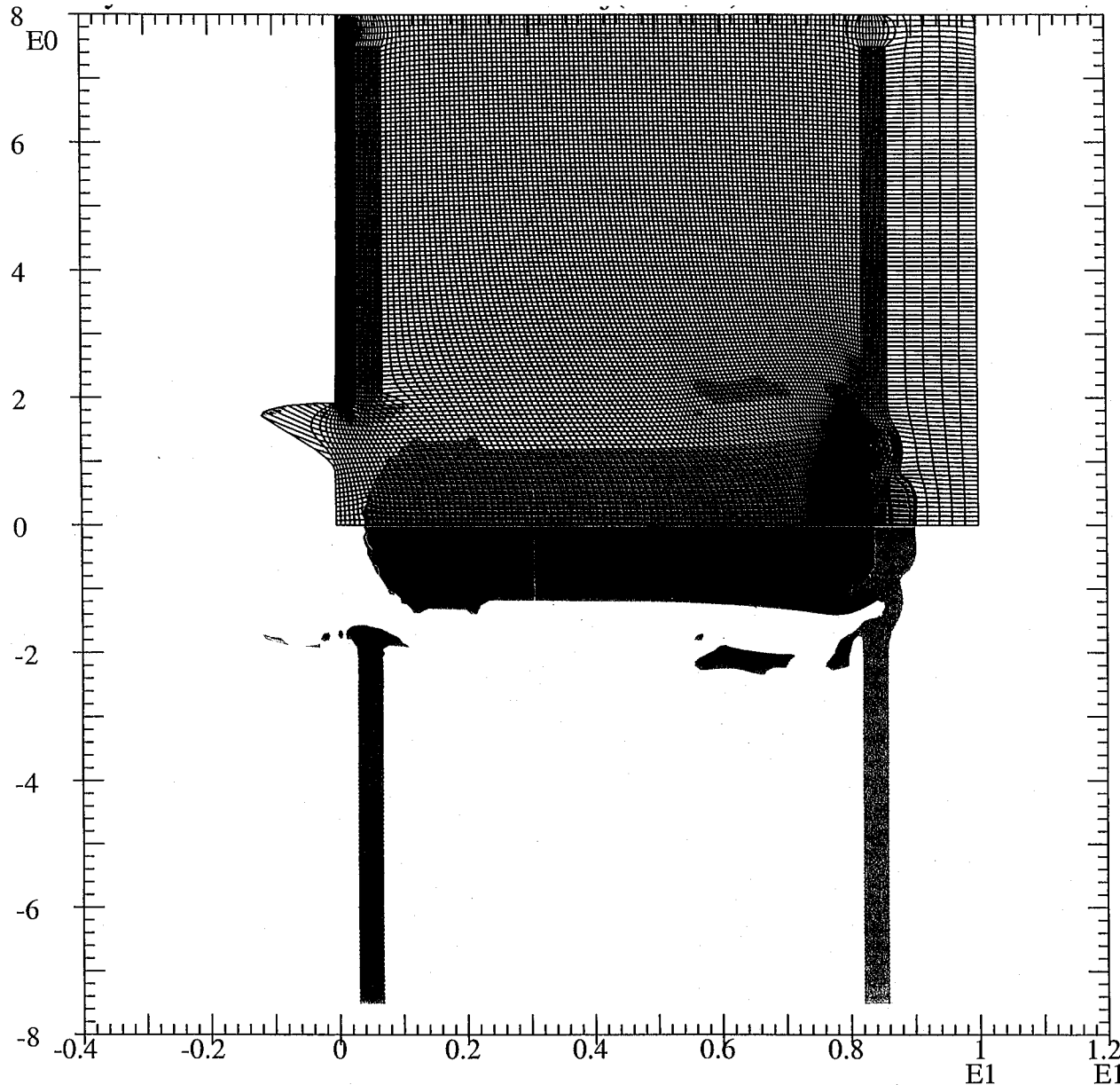
Figure 12

First series NMD EOS experiments modeling calculations



17mm diameter projectile at 11km/s:t=12μs materials plot and zoning

17



Red: projectile
Green: target
Blue: witness plate
Yellow: vacuum
background

nmda--9-mg-6-18-2001

Figure 13

First series NMD EOS experiments modeling calculations



17mm diameter projectile at 11km/s

Particle velocities at rear of witness plate on axis and 2,4 and 6mm away

18

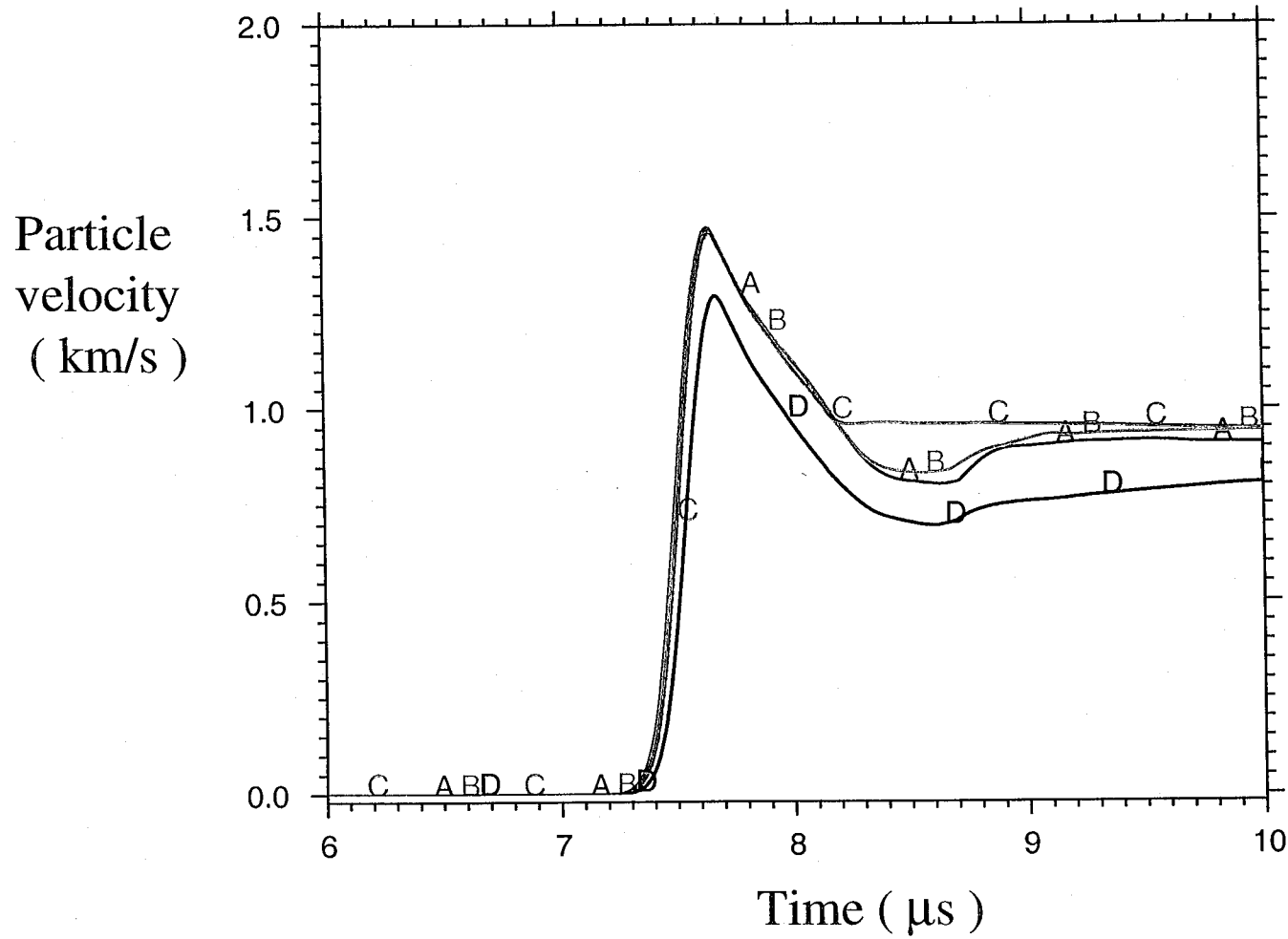


Figure 14

Second series NMD EOS experiments modeling calculations



Standard zoning (150x113) 17mm dia. proj. materials plot and zoning

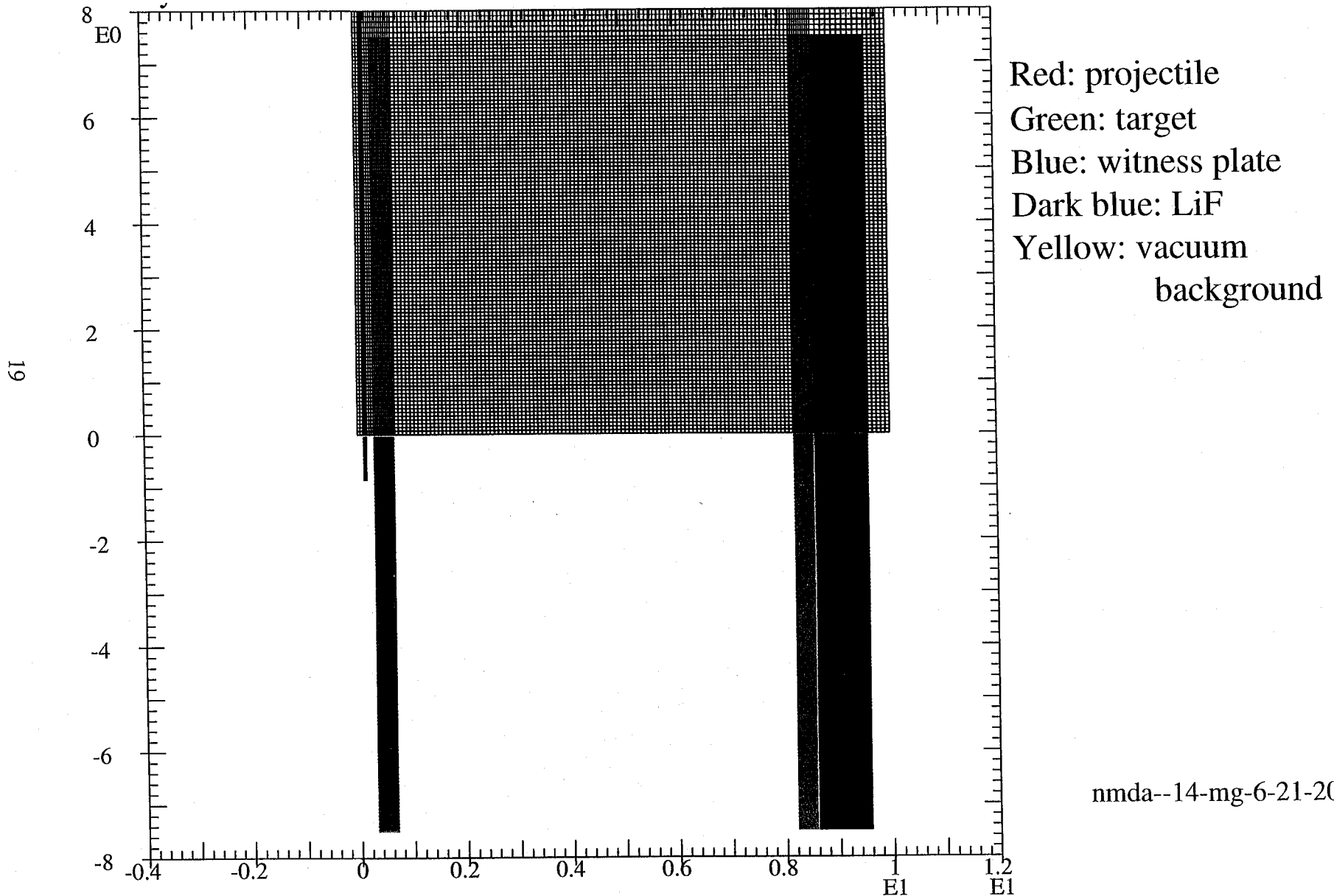


Figure 15

Second series NMD EOS experiments modeling calculations



Standard zoning (150x113) 17mm diameter projectile closeup

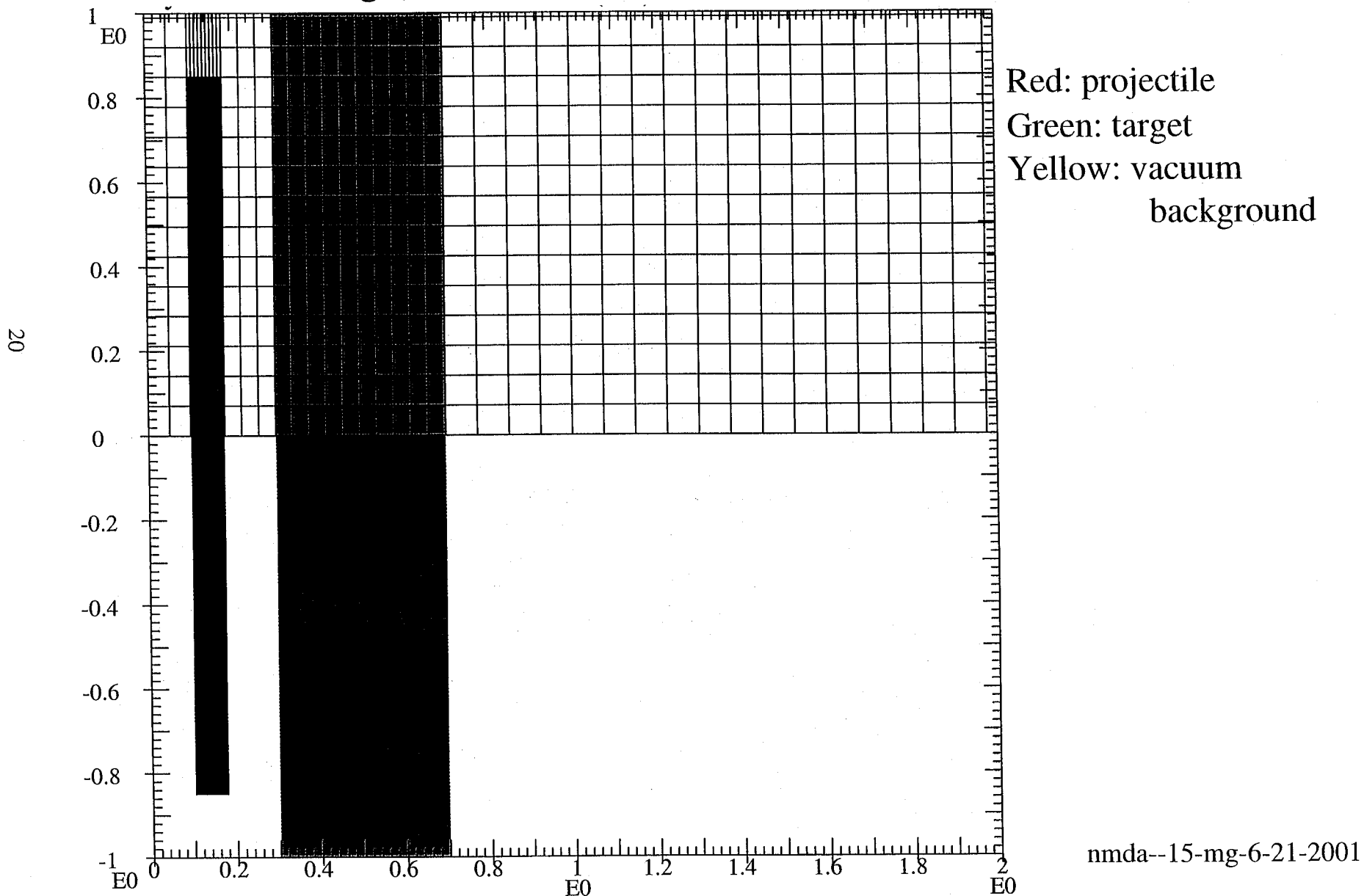


Figure 16

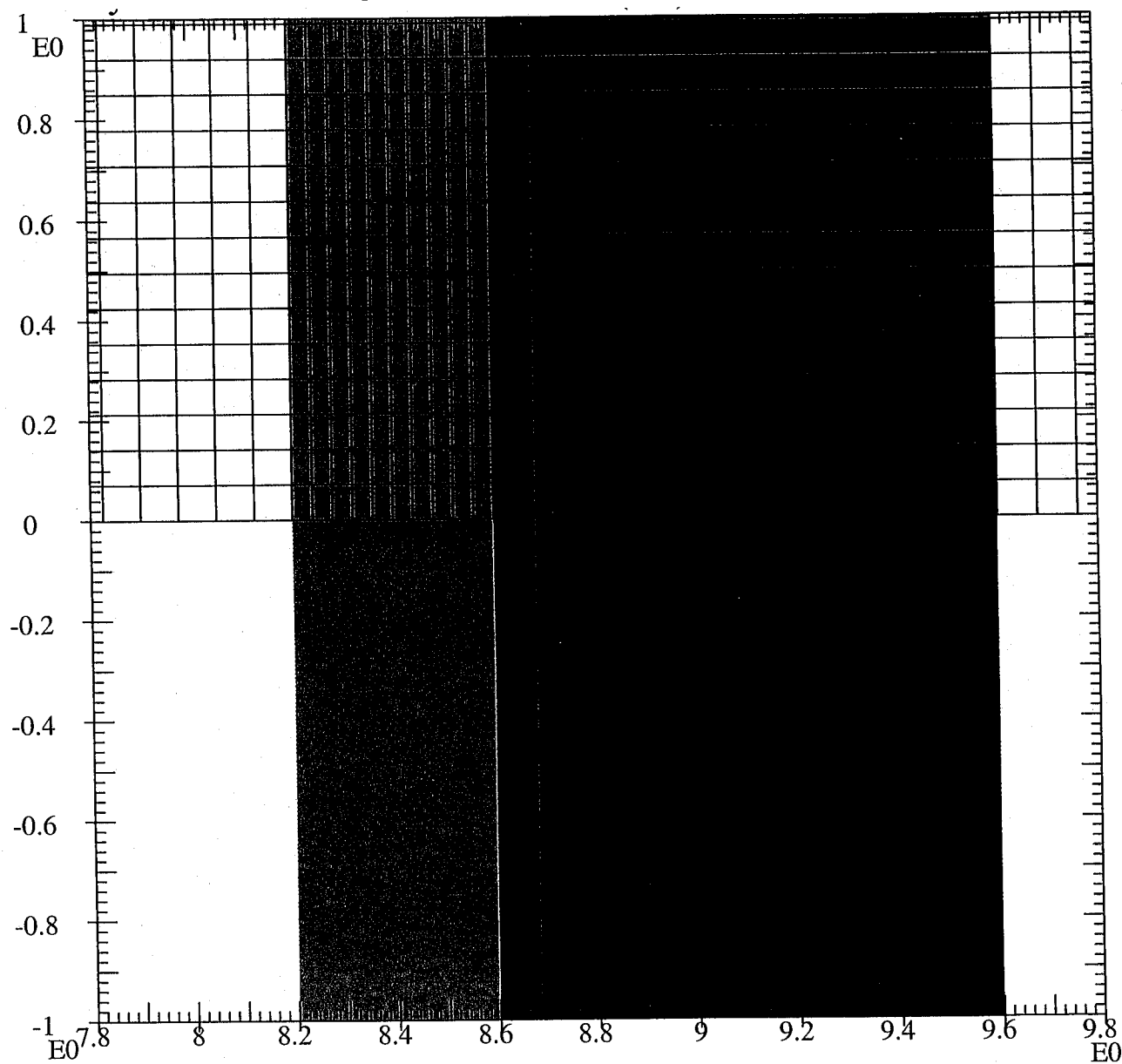
nmda--15-mg-6-21-2001

Second series NMD EOS experiments modeling calculations



Standard zoning (150x113) closeup of witness plate and backing

21



Blue: witness plate
Dark blue: LiF
Yellow: vacuum
background

nmda--16-mg-6-21-2001

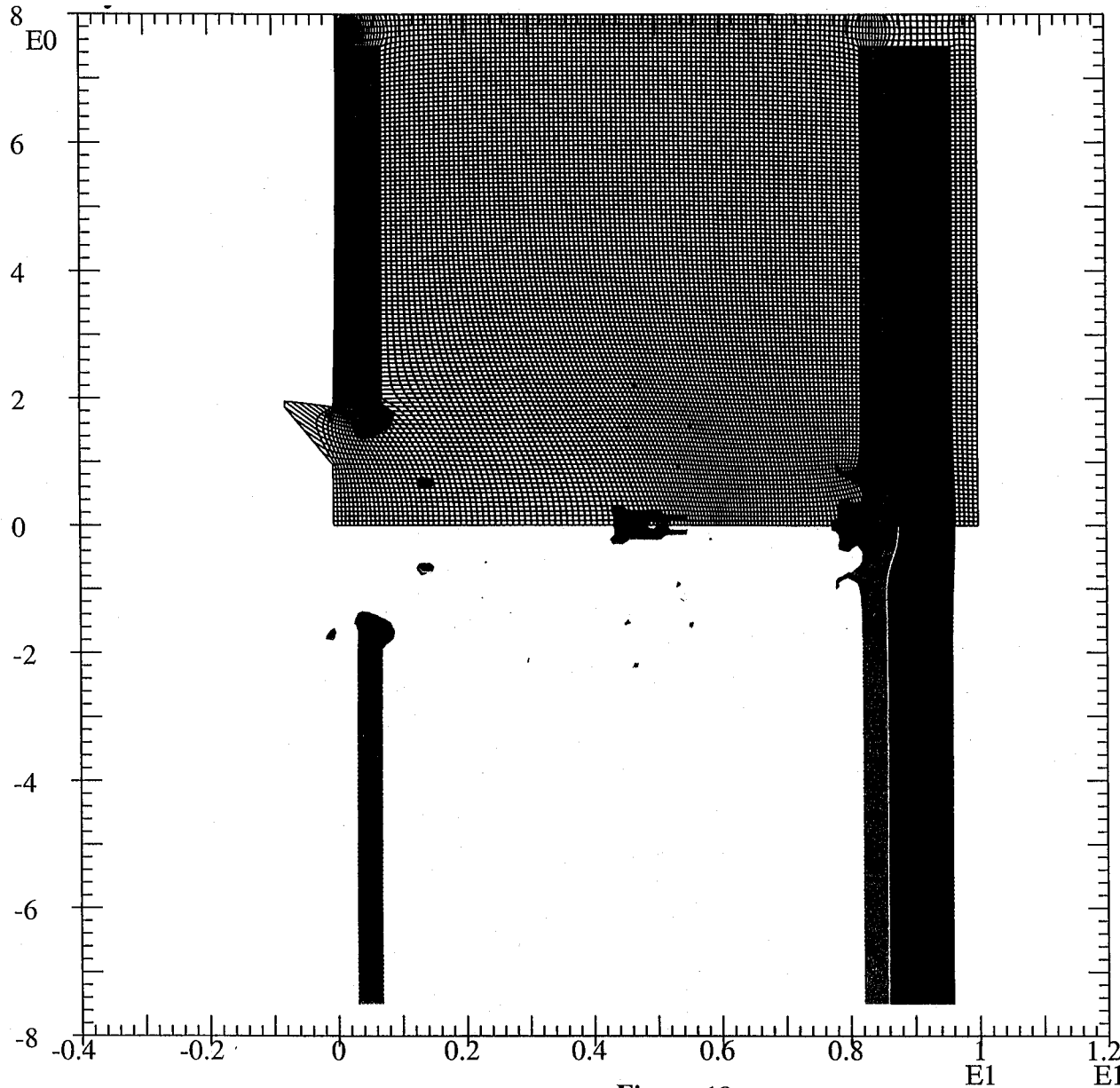
Figure 17

Second series NMD EOS experiments modeling calculations



Standard zoning (150x113) 17mm dia. proj. at 6km/s: $t=20\mu\text{s}$

22



Red: projectile
Green: target
Blue: witness plate
Dark blue: LiF
Yellow: vacuum
background

nmda--17-mg-6-21-2001

Figure 18

Second series NMD EOS experiments modeling calculations



Standard zoning (150x113) 17mm diameter projectile at 6km/s

Particle velocities at rear of witness plate on axis and 2,4 and 6mm away

23

Particle
velocity
(km/s)

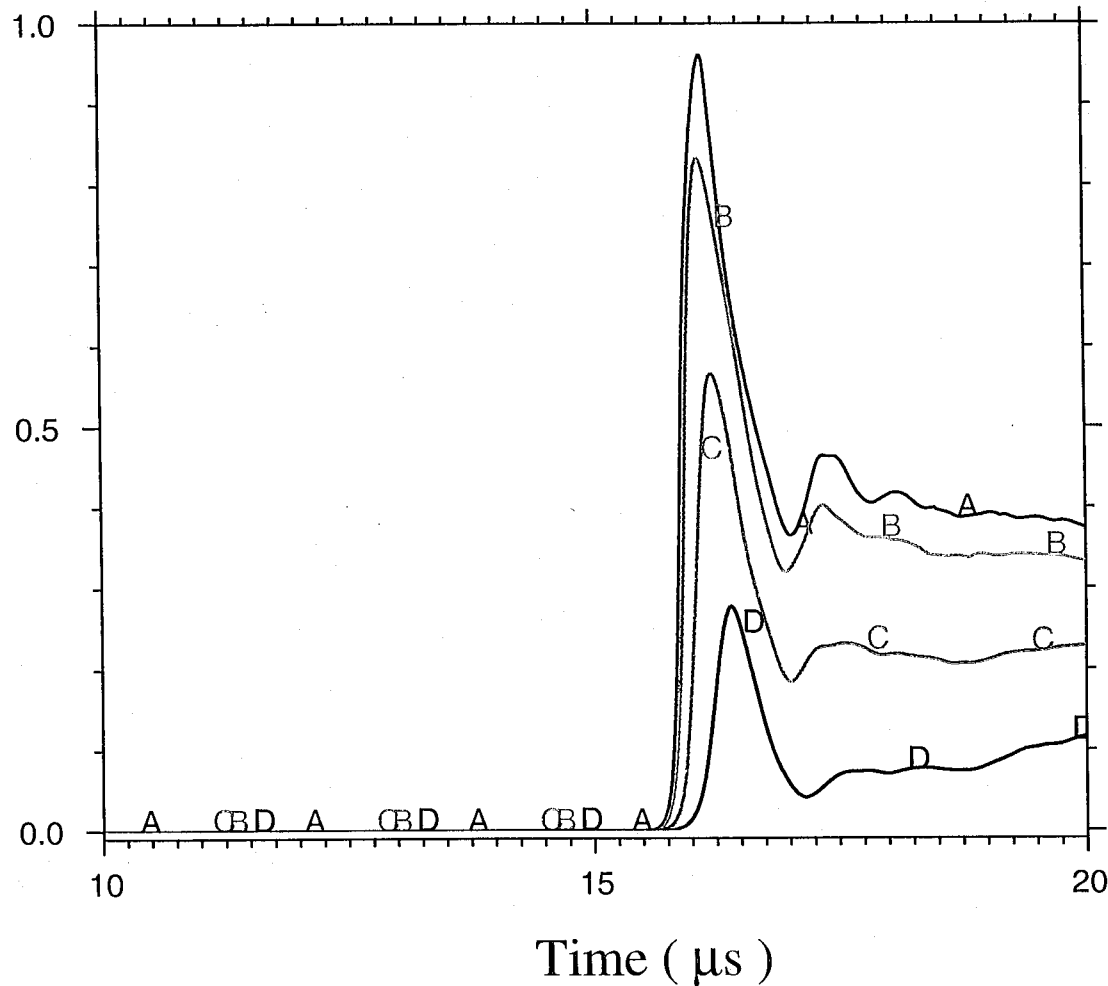


Figure 19

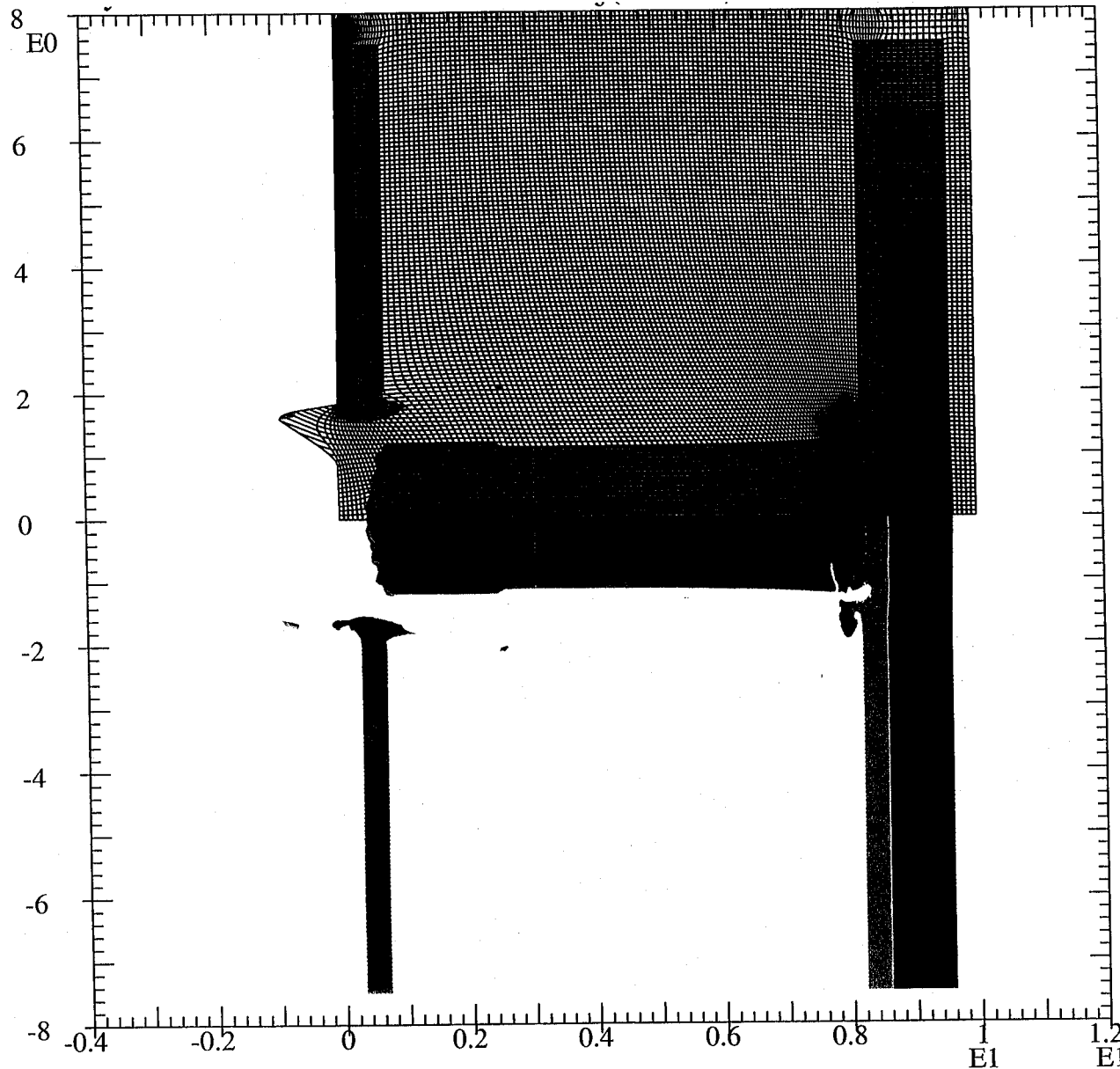
nmda--18-mg-6-21-2001

Second series NMD EOS experiments modeling calculations



Standard zoning (150x113) 17mm dia. proj. at 11km/s: $t=10\mu\text{s}$

24



Red: projectile
Green: target
Blue: witness plate
Dark blue: LiF
Yellow: vacuum
background

nmda--19-mg-6-21-2001

Figure 20

Second series NMD EOS experiments modeling calculations



Standard zoning (150x113) 17mm diameter projectile at 11km/s

Particle velocities at rear of witness plate on axis and 2,4 and 6mm away

25

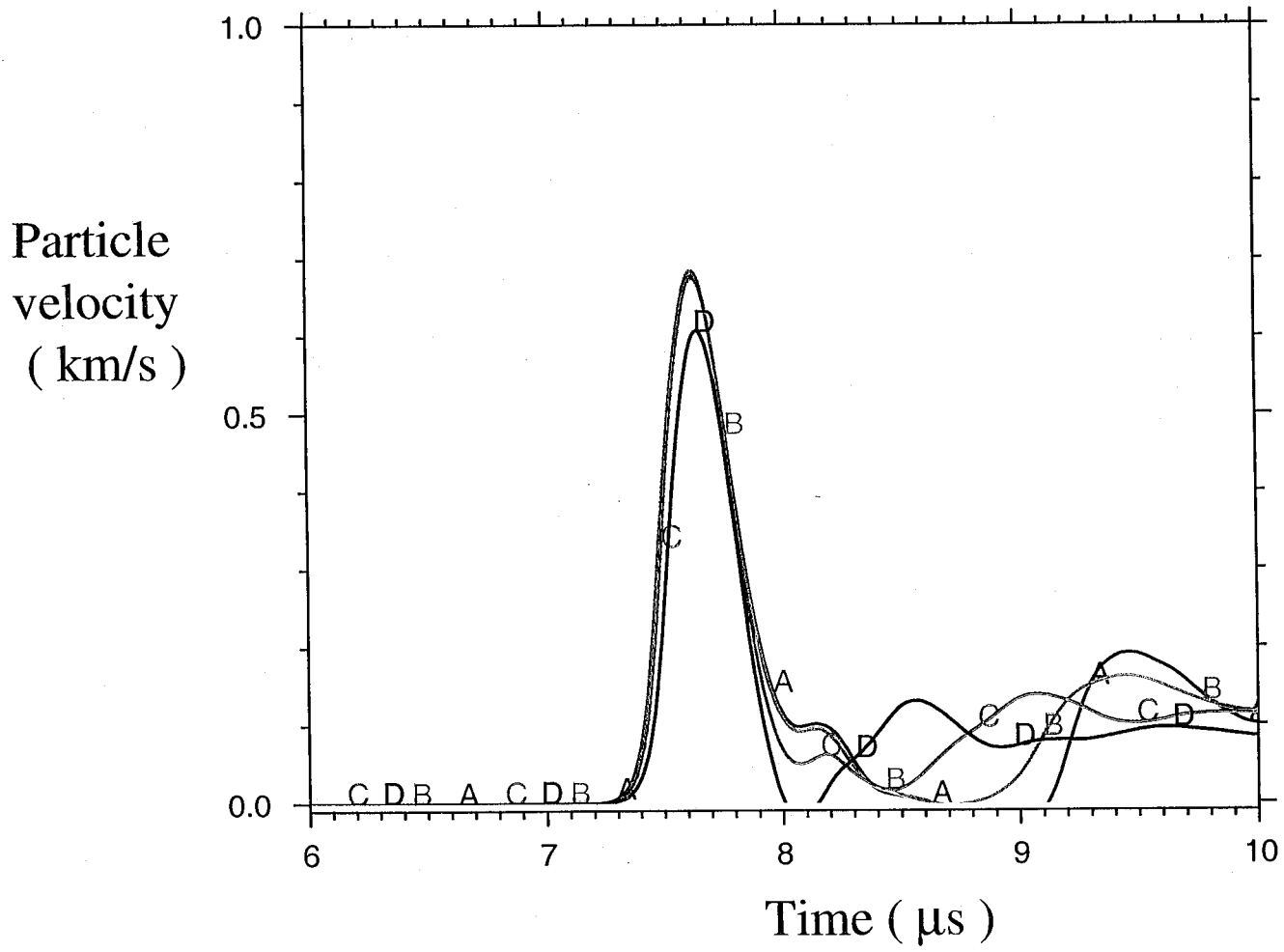
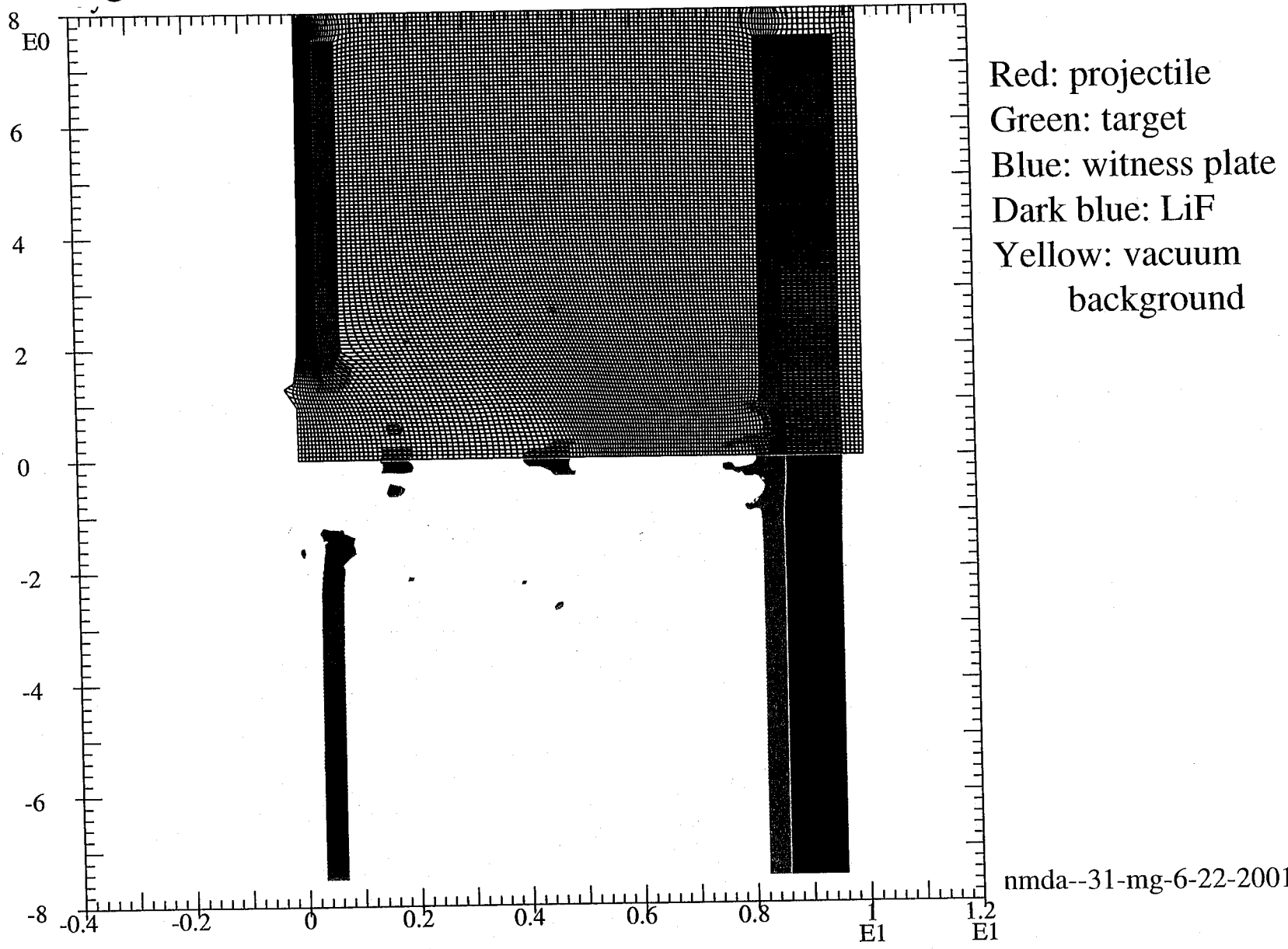


Figure 21

Second series NMD EOS experiments modeling calculations

St. zoning (150x113) 17mm dia. proj. at 6km/s target strength X2: $t=22\mu\text{s}$

26



nmda--31-mg-6-22-2001

Figure 22

Second series NMD EOS experiments modeling calculations

Standard zoning (150x113) 17mm dia. proj. 6km/s target strength X2
Particle velocities at rear of witness plate on axis and 2,4 and 6mm away

27

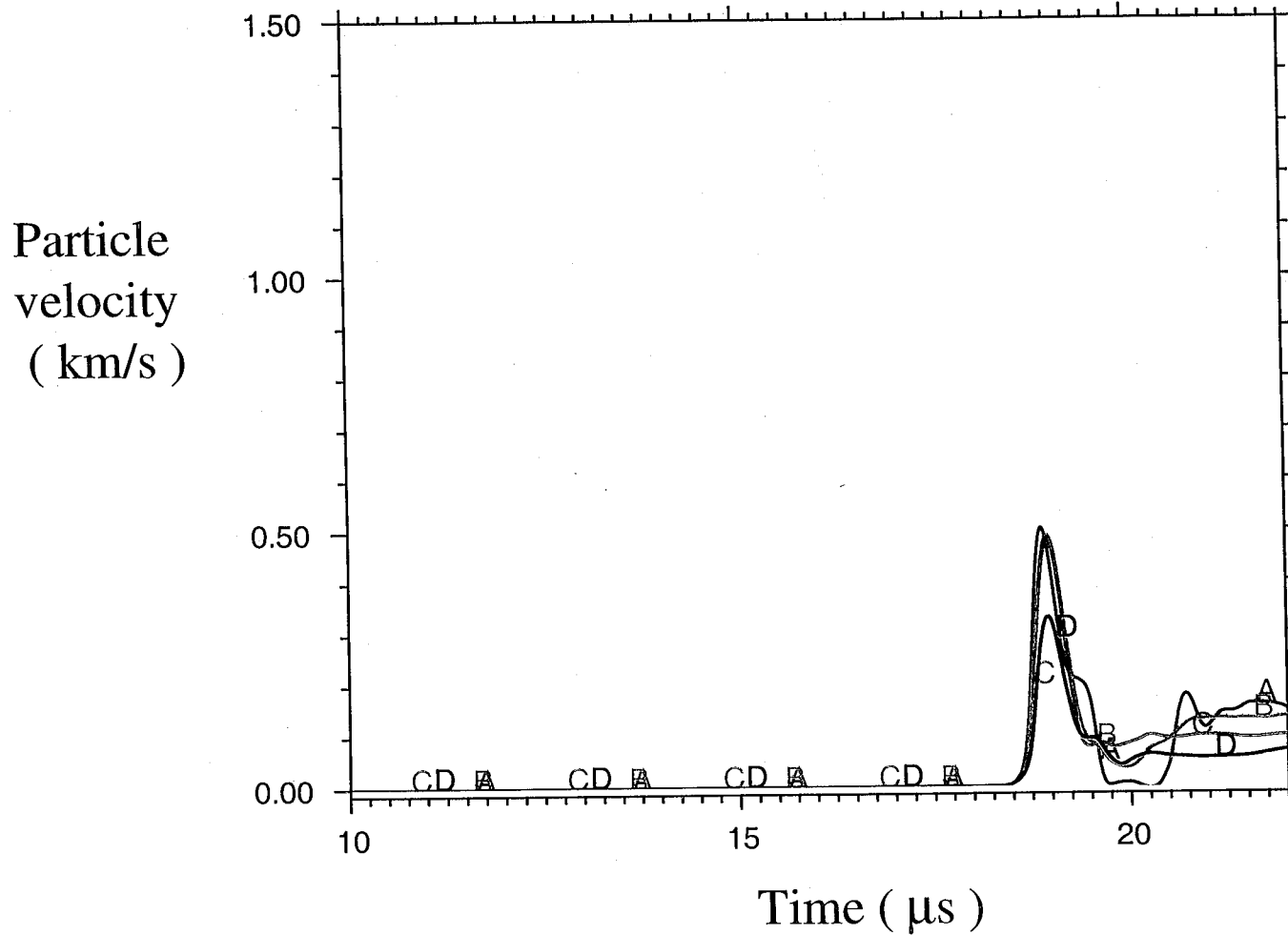
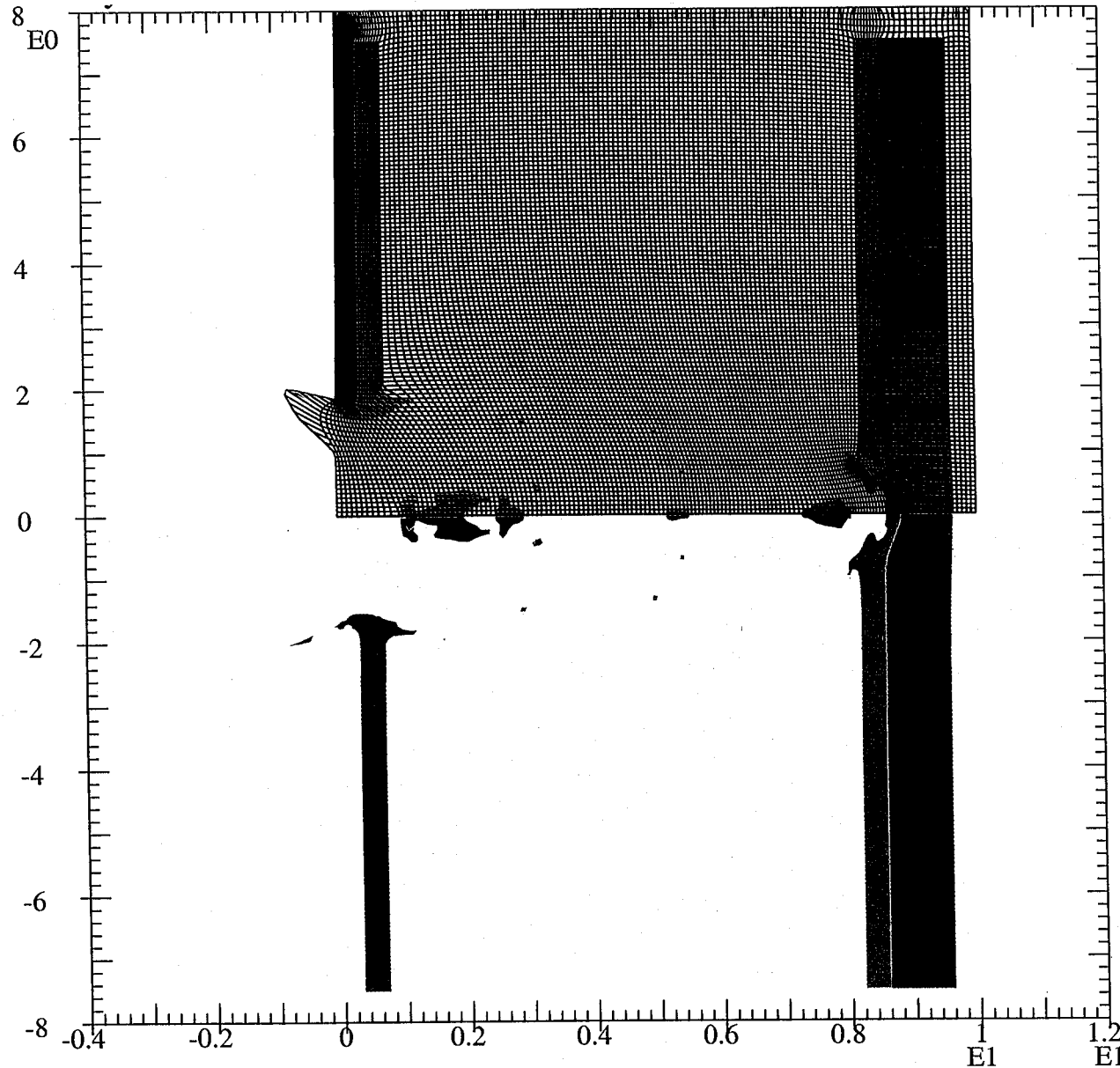


Figure 23

Second series NMD EOS experiments modeling calculations

St. zoning (150x113) 17mm dia. proj. at 6km/s target strength X0.5: $t=20\mu\text{s}$



Red: projectile
Green: target
Blue: witness plate
Dark blue: LiF
Yellow: vacuum
background

28

nmda--32-mg-6-22-2001

Figure 24

Second series NMD EOS experiments modeling calculations

Standard zoning (150x113) 17mm dia. proj. 6km/s target strength X0.5
Particle velocities at rear of witness plate on axis and 2,4 and 6mm away

29

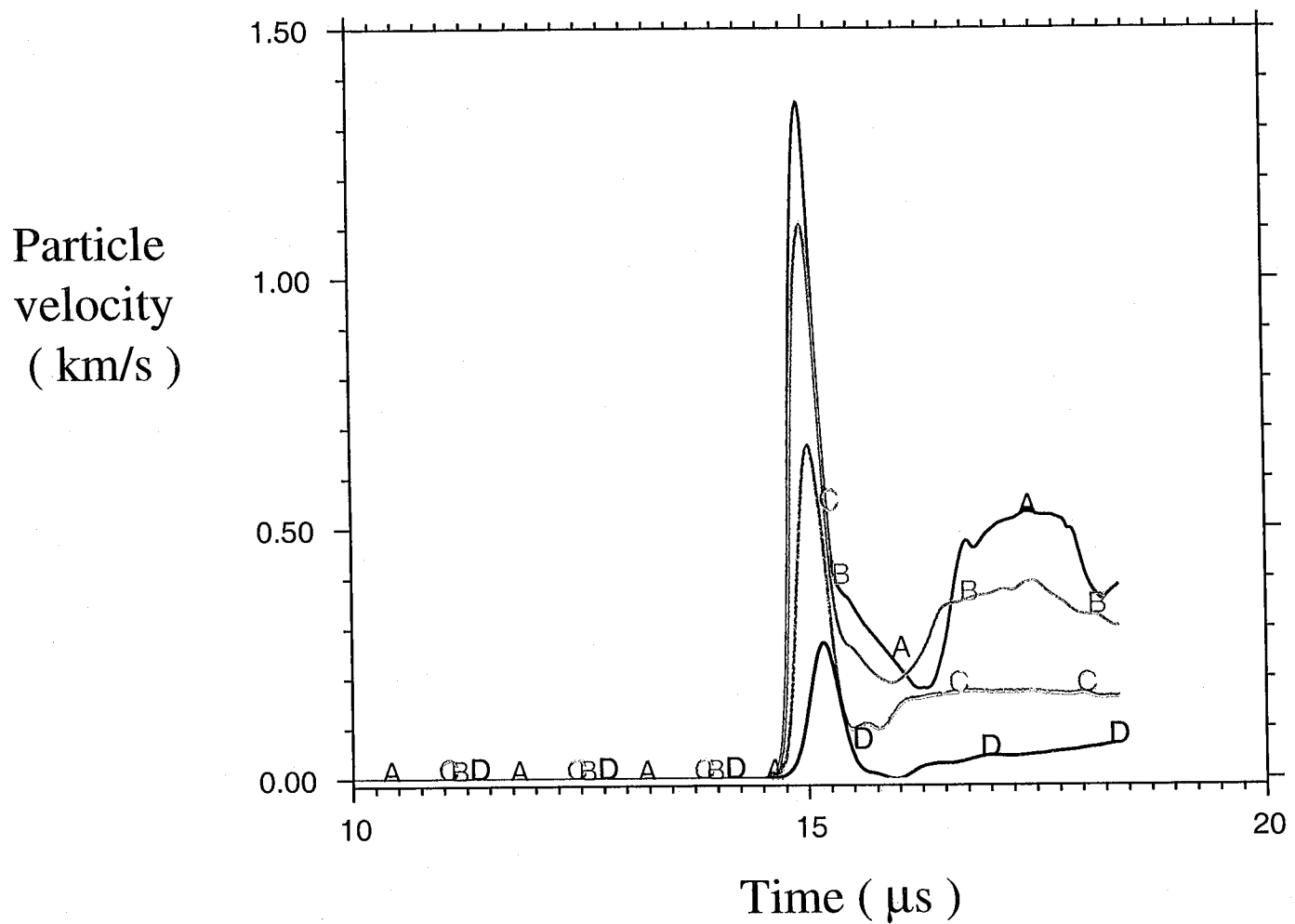


Figure 25

Second series NMD EOS experiments modeling calculations: particle velocity profile dependence on target strength



Standard zoning (150x113) 17mm diameter projectile 6km/s

Particle velocities at rear of witness plate on axis and 2,4 and 6mm away

Early large peaks for target strength X0.5, late small ones for target strength X2

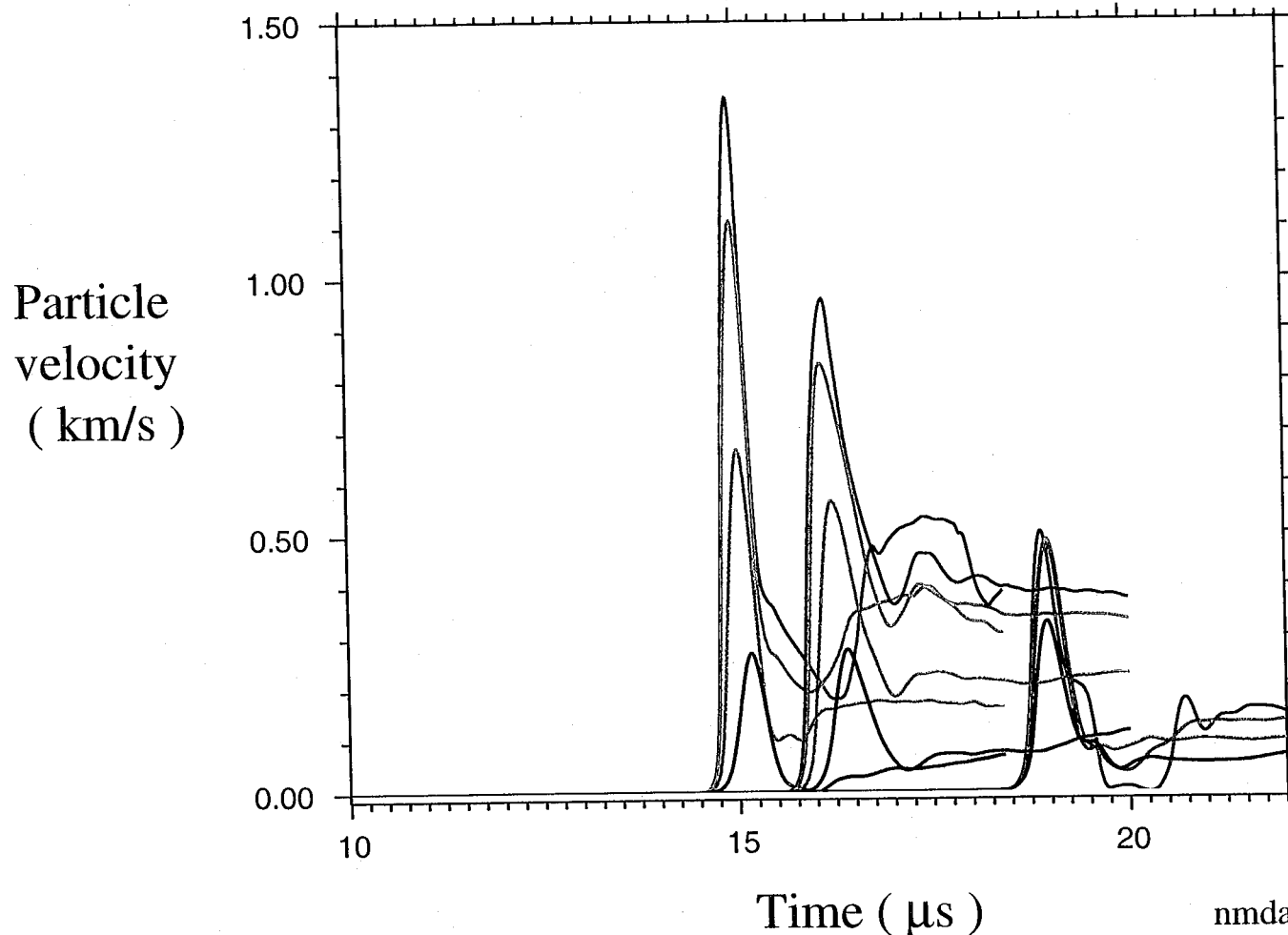
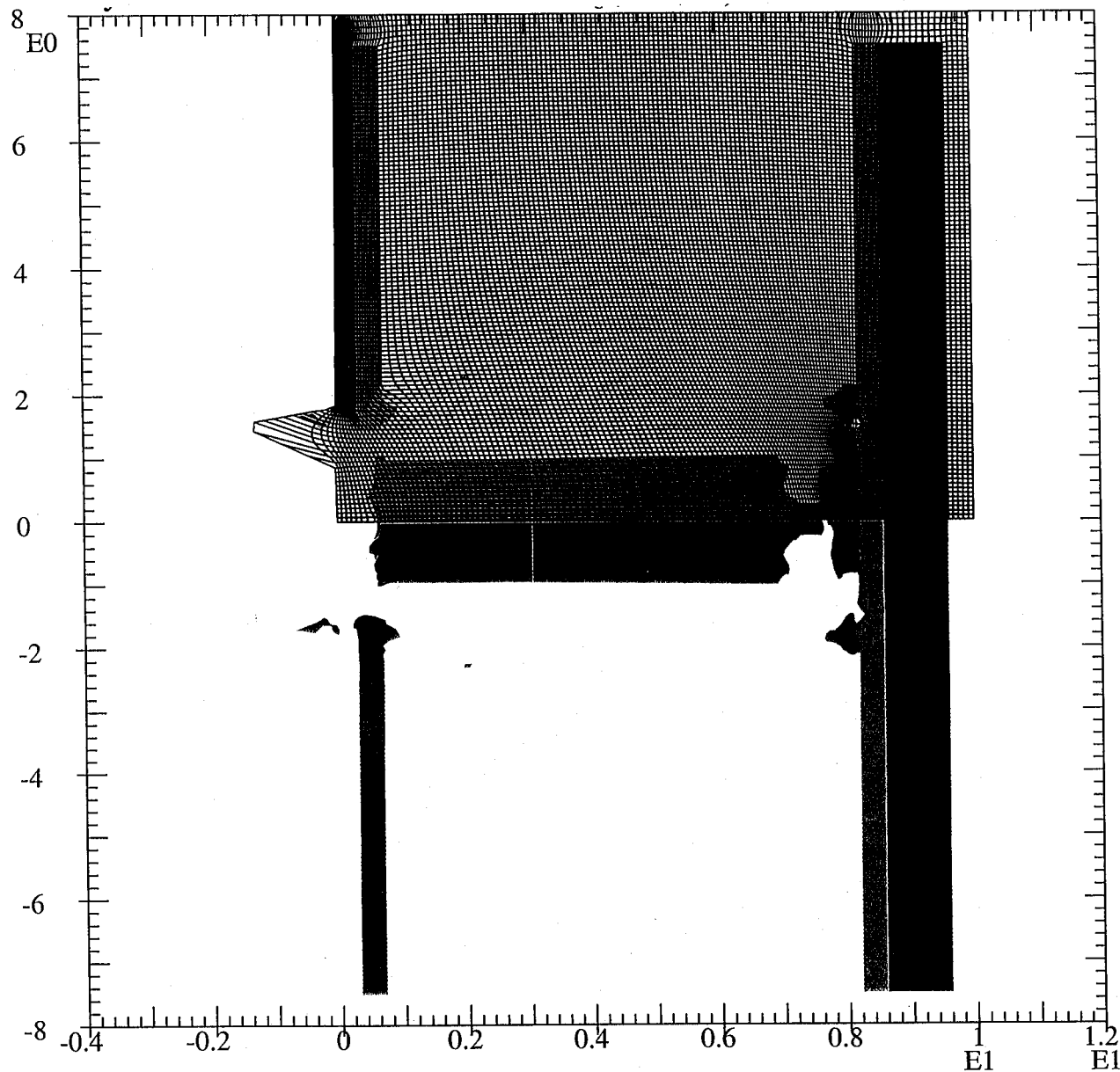


Figure 26

Second series NMD EOS experiments modeling calculations

St. zoning (150x113) 17mm dia. proj. 11km/s target strength X2: $t=11\mu\text{s}$



Red: projectile
Green: target
Blue: witness plate
Dark blue: LiF
Yellow: vacuum
background

Figure 27

nmda--33-mg-7-2-2001

Second series NMD EOS experiments modeling calculations 
Standard zoning (150x113) 17mm dia. proj. 11km/s target strength X2
Particle velocities at rear of witness plate on axis and 2,4 and 6mm away

32

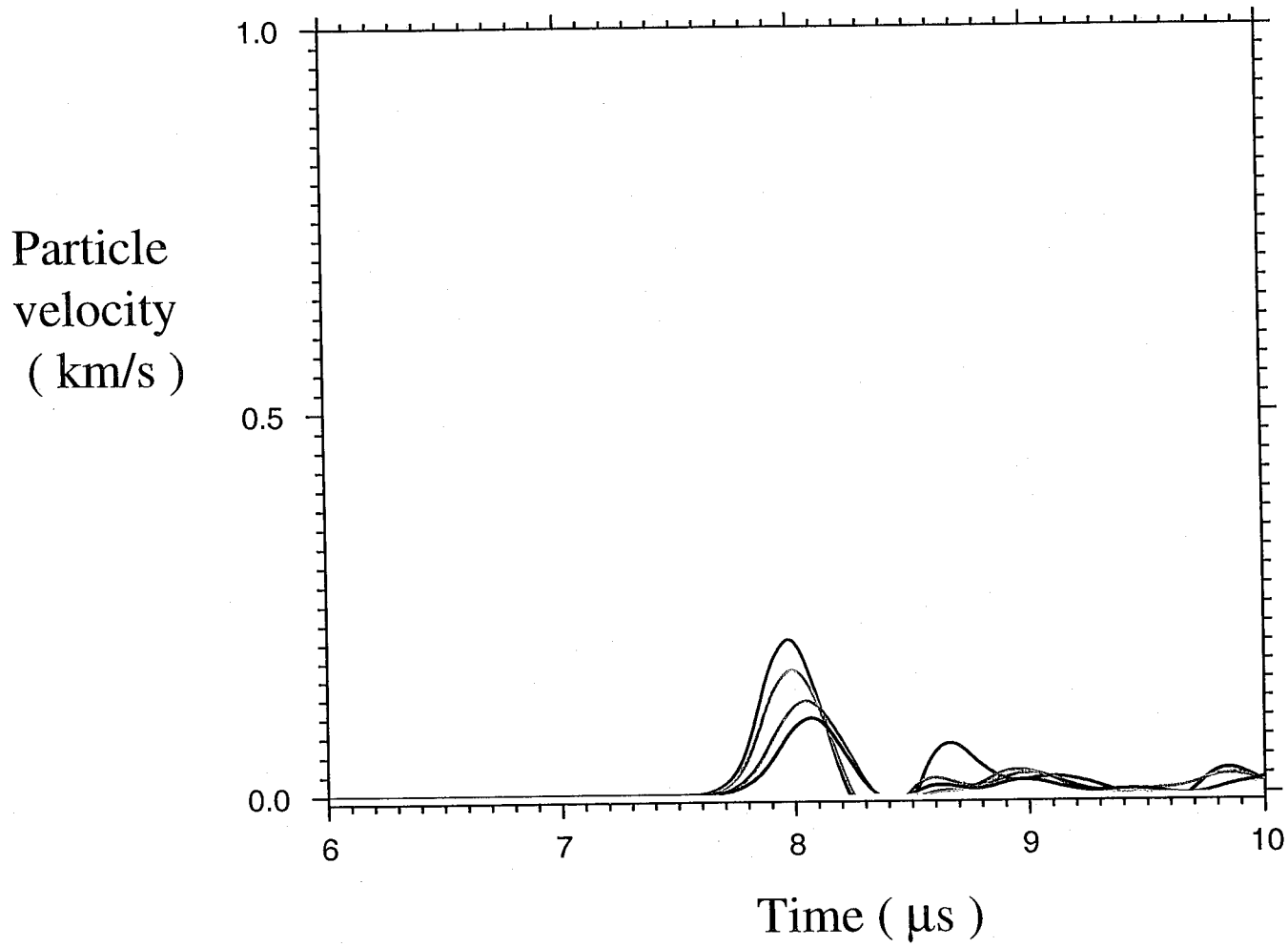
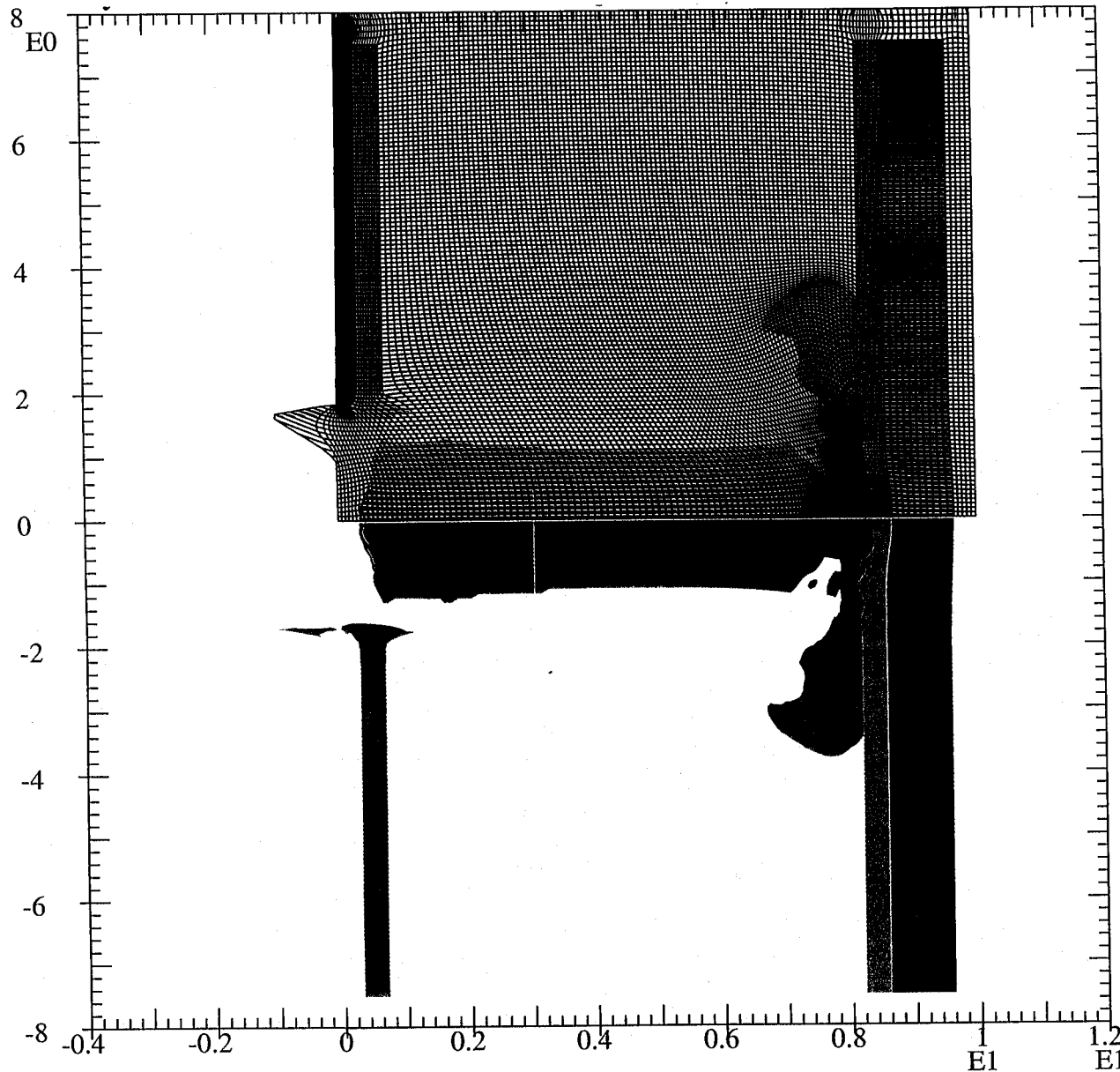


Figure 28

Second series NMD EOS experiments modeling calculations

St. zoning (150x113) 17mm dia. proj. 11km/s target strength X0.5: $t=10\mu\text{s}$



Red: projectile
Green: target
Blue: witness plate
Dark blue: LiF
Yellow: vacuum
background

33

nmda--35-mg-7-2-2001

Figure 29

Second series NMD EOS experiments modeling calculations



Standard zoning (150x113) 17mm dia. proj. 11km/s target strength X0.5
Particle velocities at rear of witness plate on axis and 2,4 and 6mm away

34

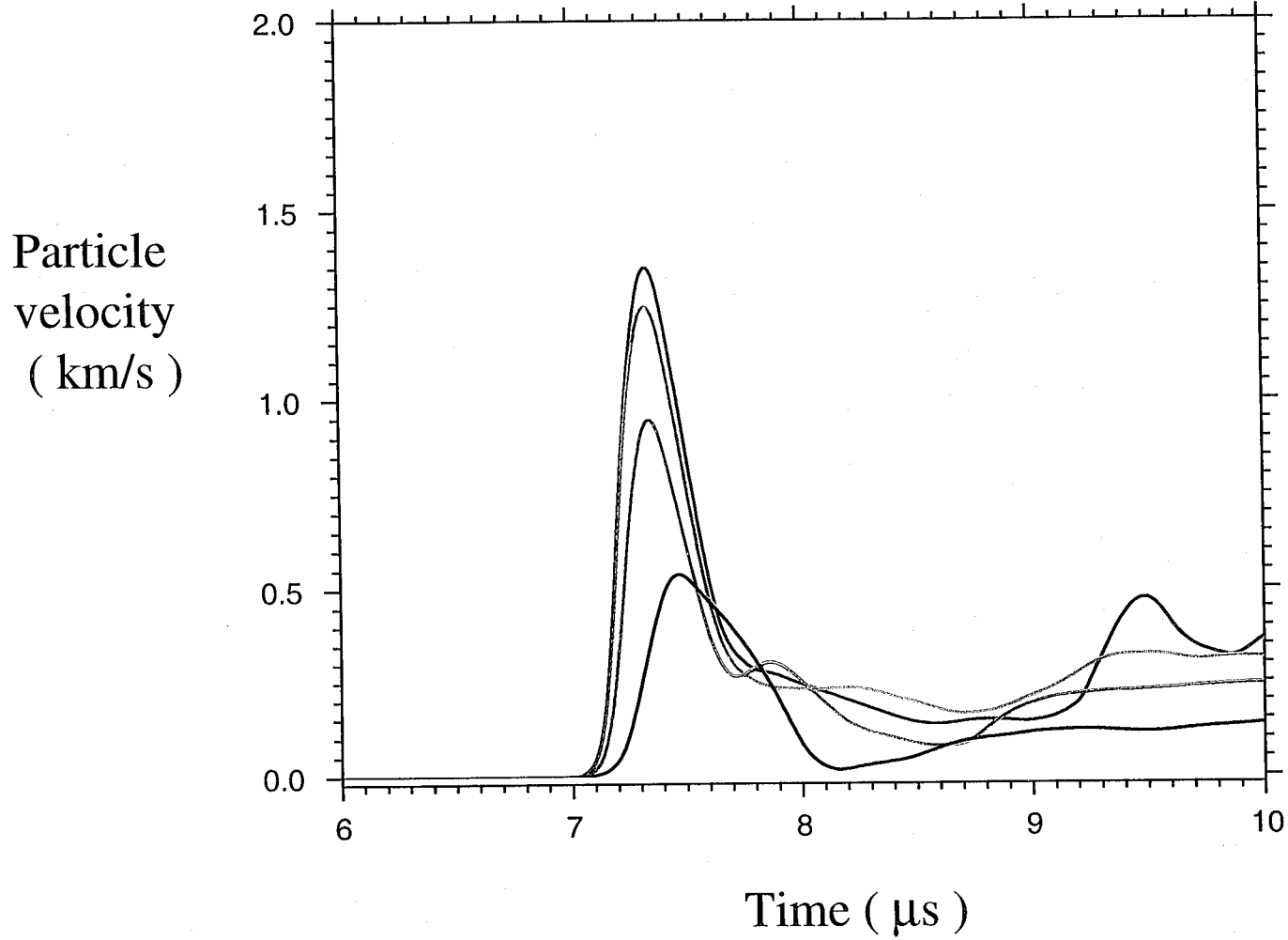


Figure 30

Second series NMD EOS experiments modeling calculations: particle velocity profile dependence on target strength



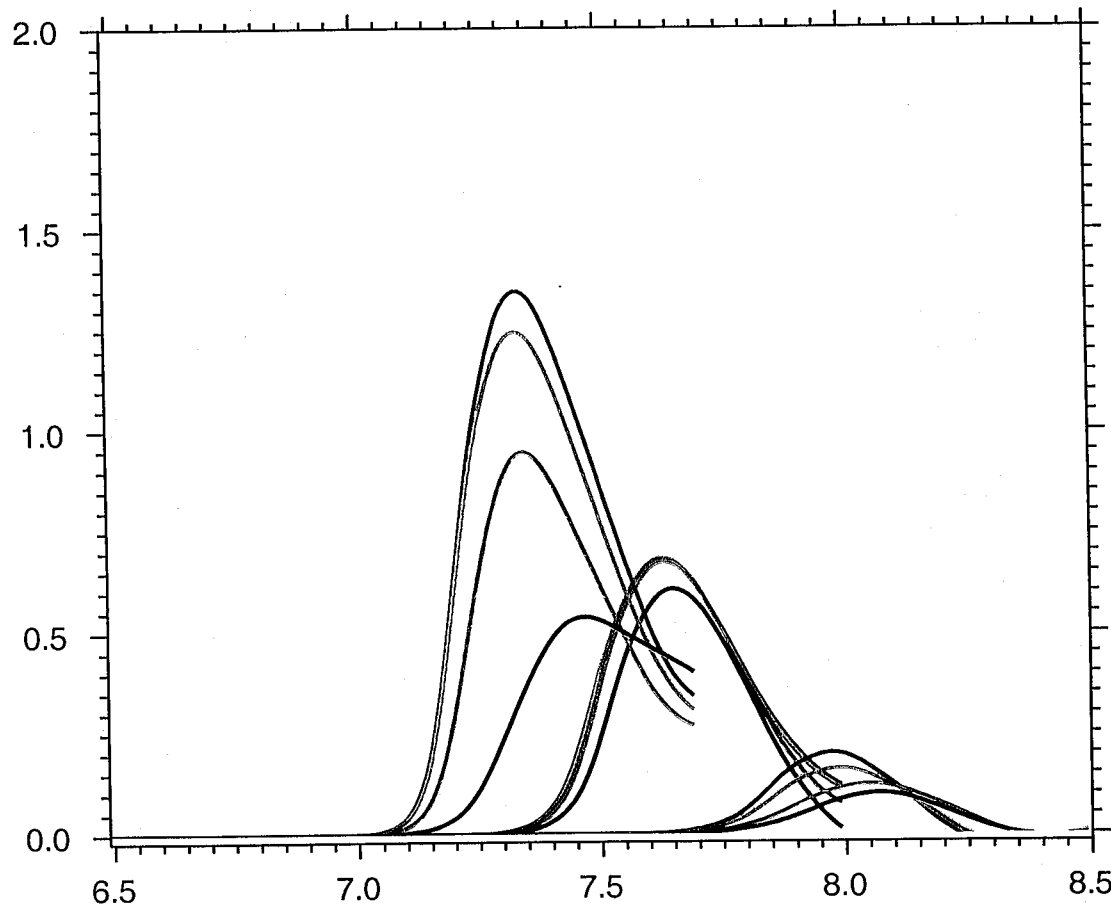
Standard zoning (150x113) 17mm diameter projectile 11km/s

Particle velocities at rear of witness plate on axis and 2,4 and 6mm away

Early large peaks for target strength X0.5, late small ones for target strength X2

35

Particle
velocity
(km/s)



Time (μ s)

Figure 31

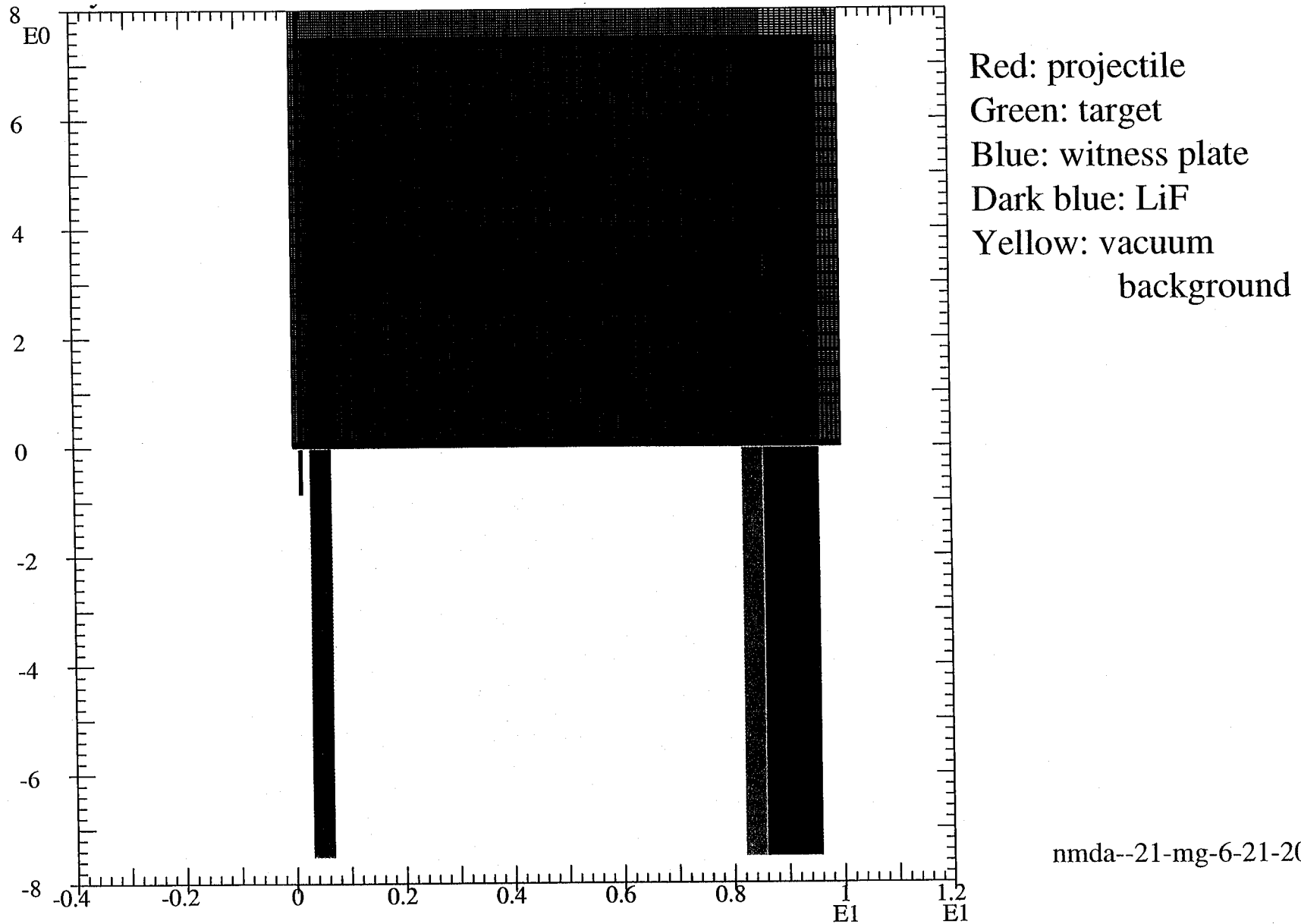
nmda--37-mg-7-2-2001

Second series NMD EOS experiments modeling calculations



Fine zoning (240x225) 17mm dia. proj. materials plot and zoning

36



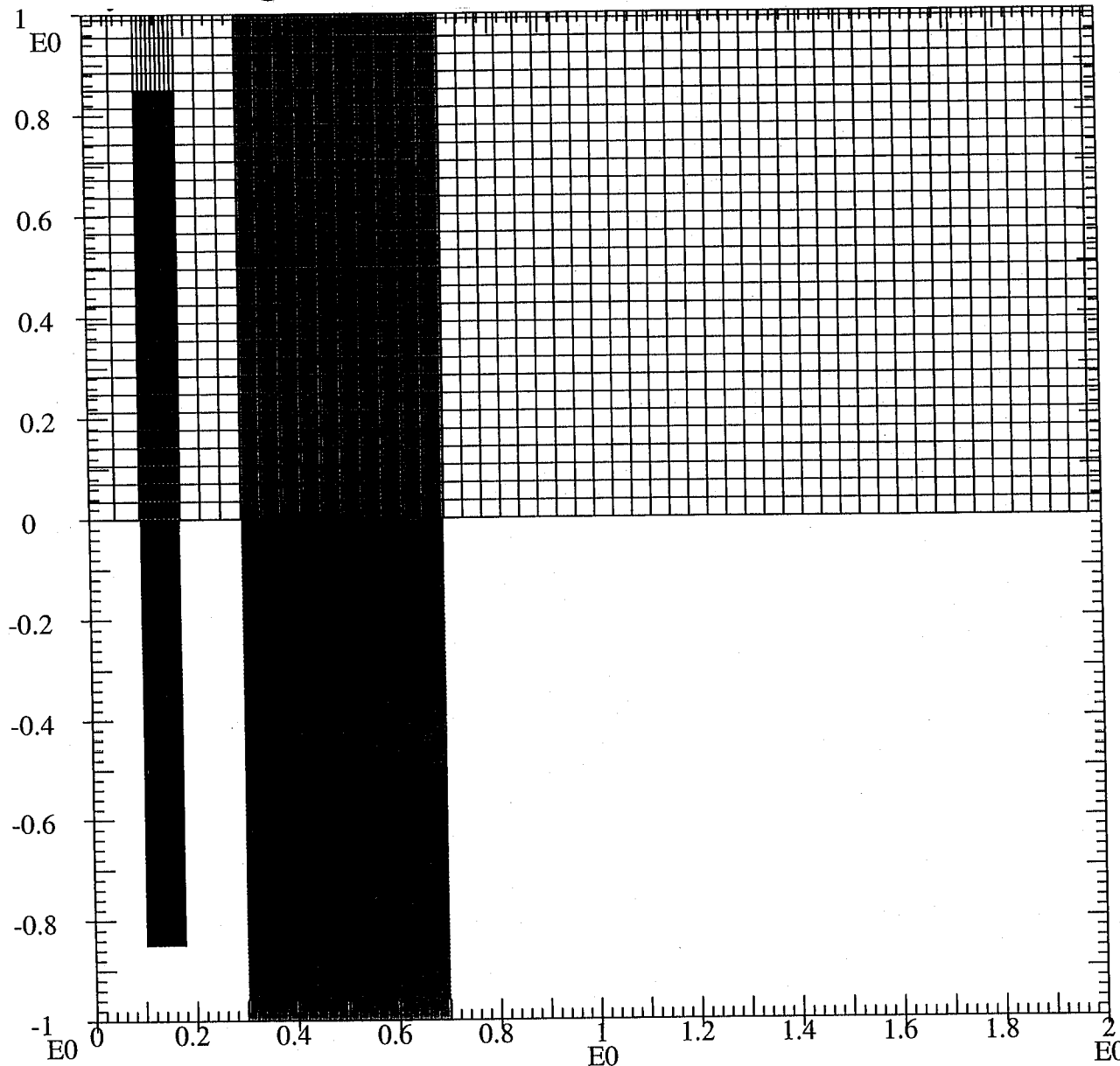
nmda--21-mg-6-21-2001

Figure 32

Second series NMD EOS experiments modeling calculations



Fine zoning (240x225) 17mm diameter projectile closeup



Red: projectile
Green: target
Yellow: vacuum
background

37

nmda--22-mg-6-21-2001

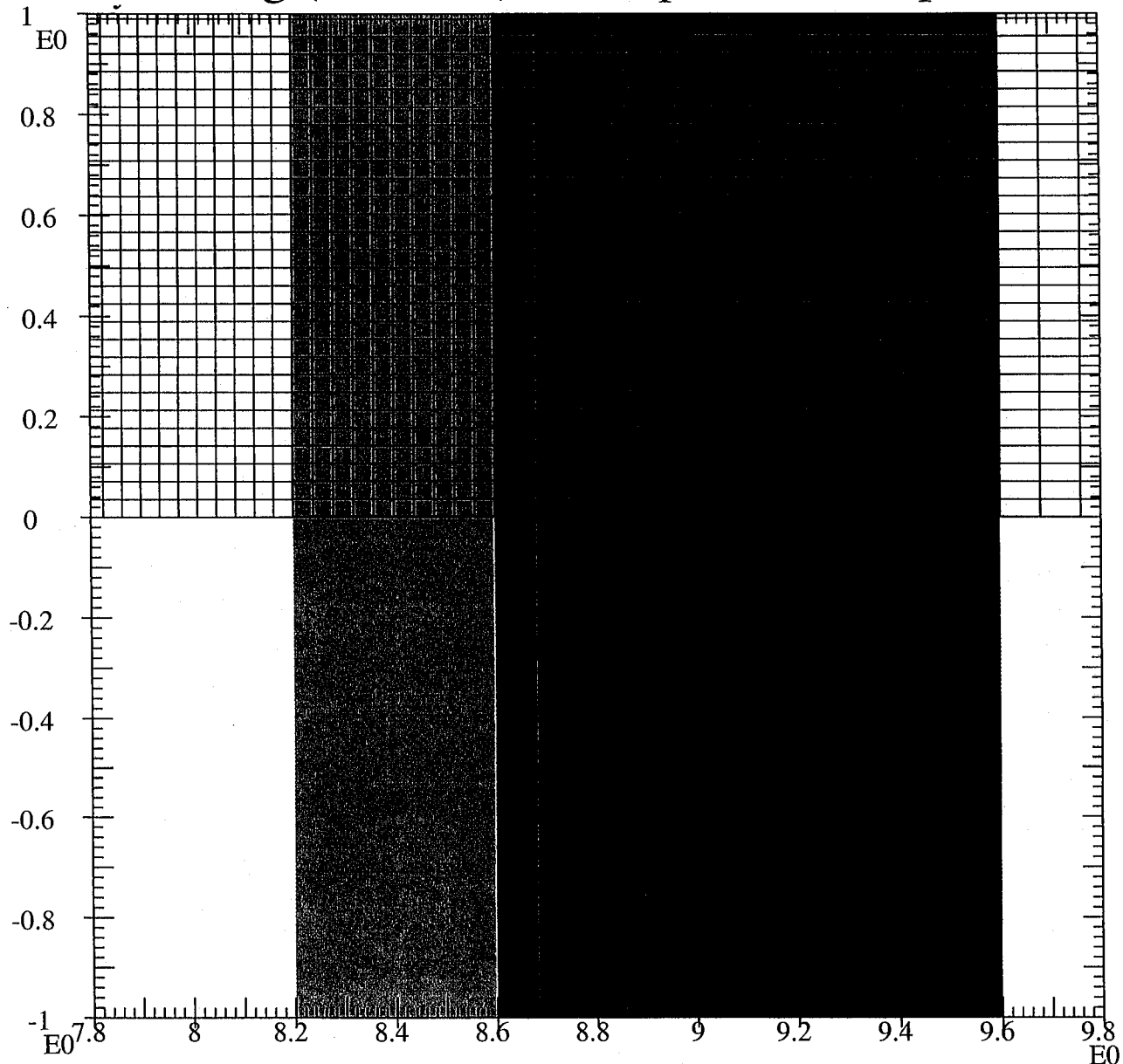
Figure 33

Second series NMD EOS experiments modeling calculations



Fine zoning (240x225) closeup of witness plate and backing

38



Blue: witness plate
Dark blue: LiF
Yellow: vacuum
background

Figure 34

nmda--23-mg-6-21-2001

Second series NMD EOS experiments modeling calculations



Fine zoning (240x225) 17mm dia. proj. at 6km/s: $t=20\mu\text{s}$

39

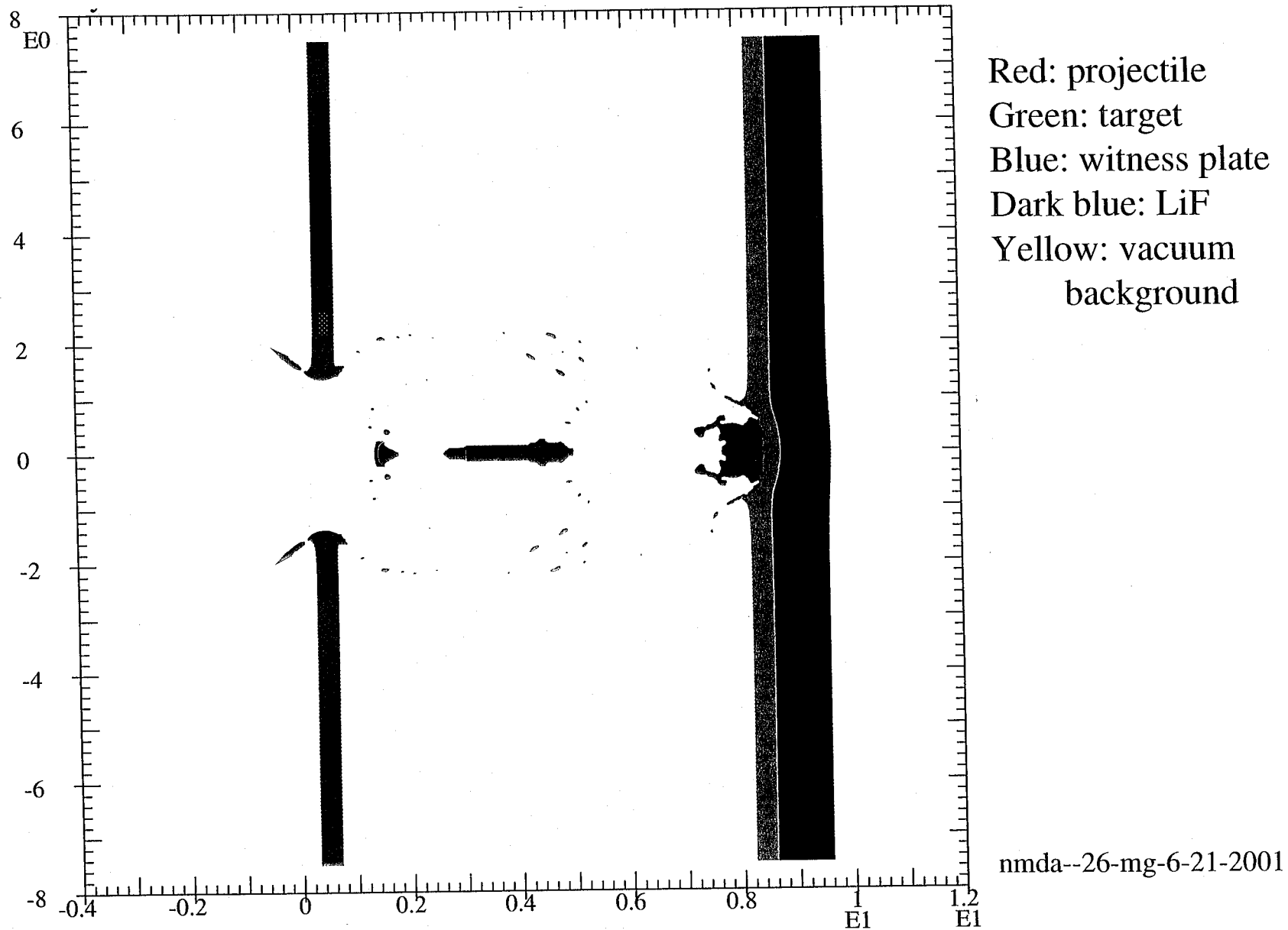


Figure 35

nmda--26-mg-6-21-2001

Second series NMD EOS experiments modeling calculations

Fine zoning (240x225) 17mm diameter projectile at 6km/s

Particle velocities at rear of witness plate on axis and 2,4 and 6mm away

40

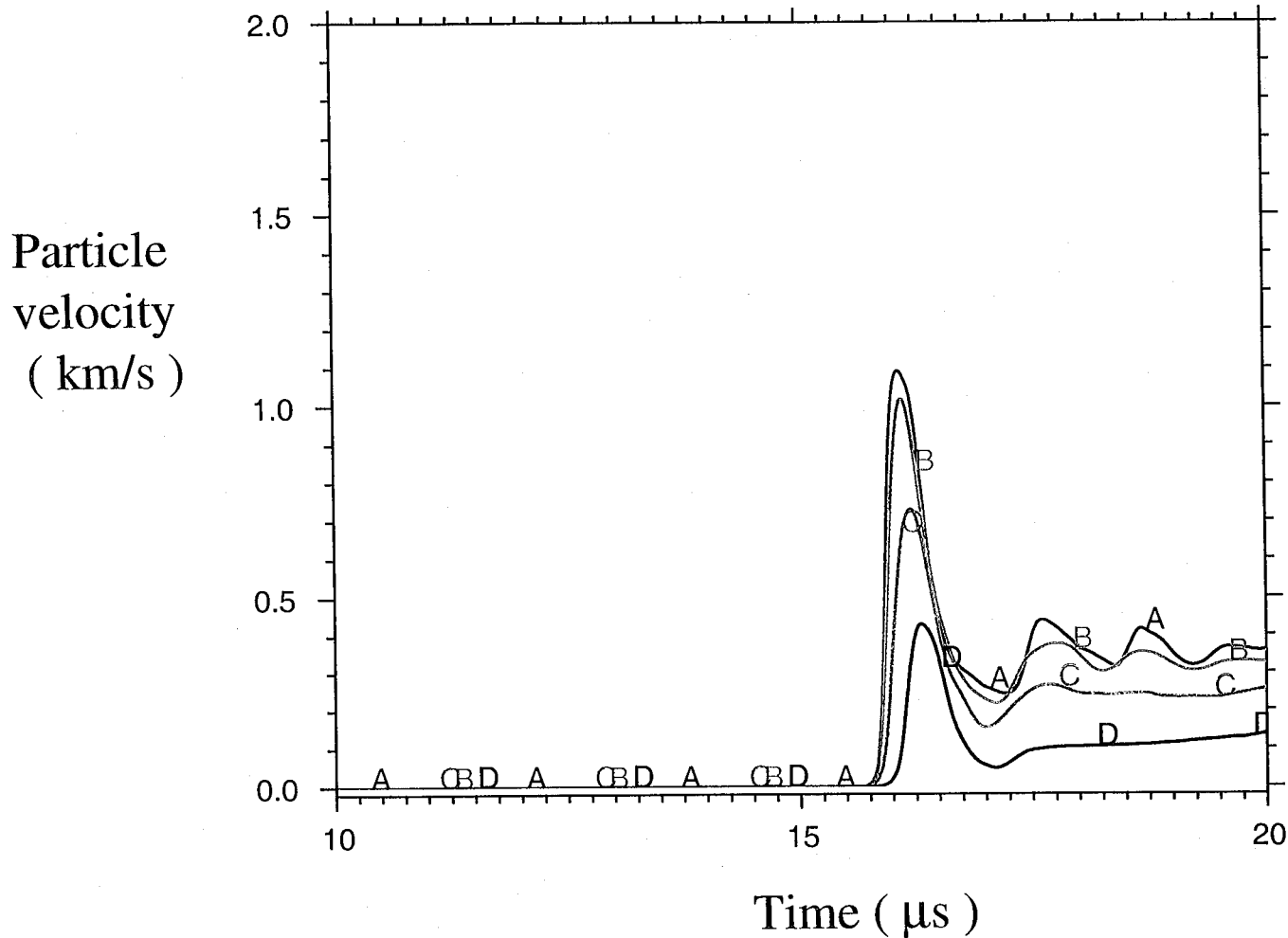


Figure 36

Second series NMD EOS experiments modeling calculations

Fine zoning (240x225) 17mm dia. proj. at 11km/s: $t=10\mu\text{s}$

41

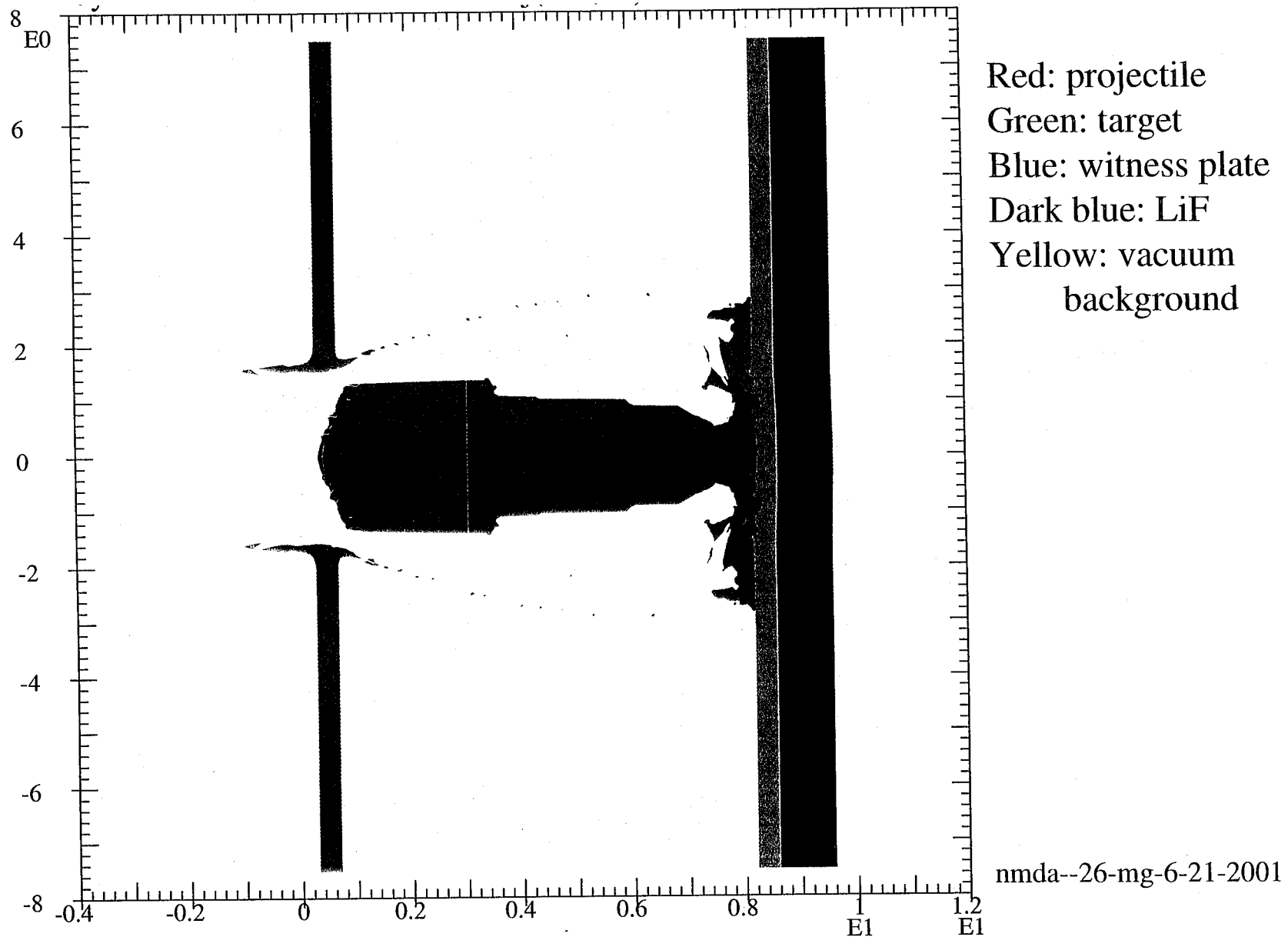


Figure 37

Second series NMD EOS experiments modeling calculations



Fine zoning (240x225) 17mm diameter projectile at 11km/s

Particle velocities at rear of witness plate on axis and 2,4 and 6mm away

42

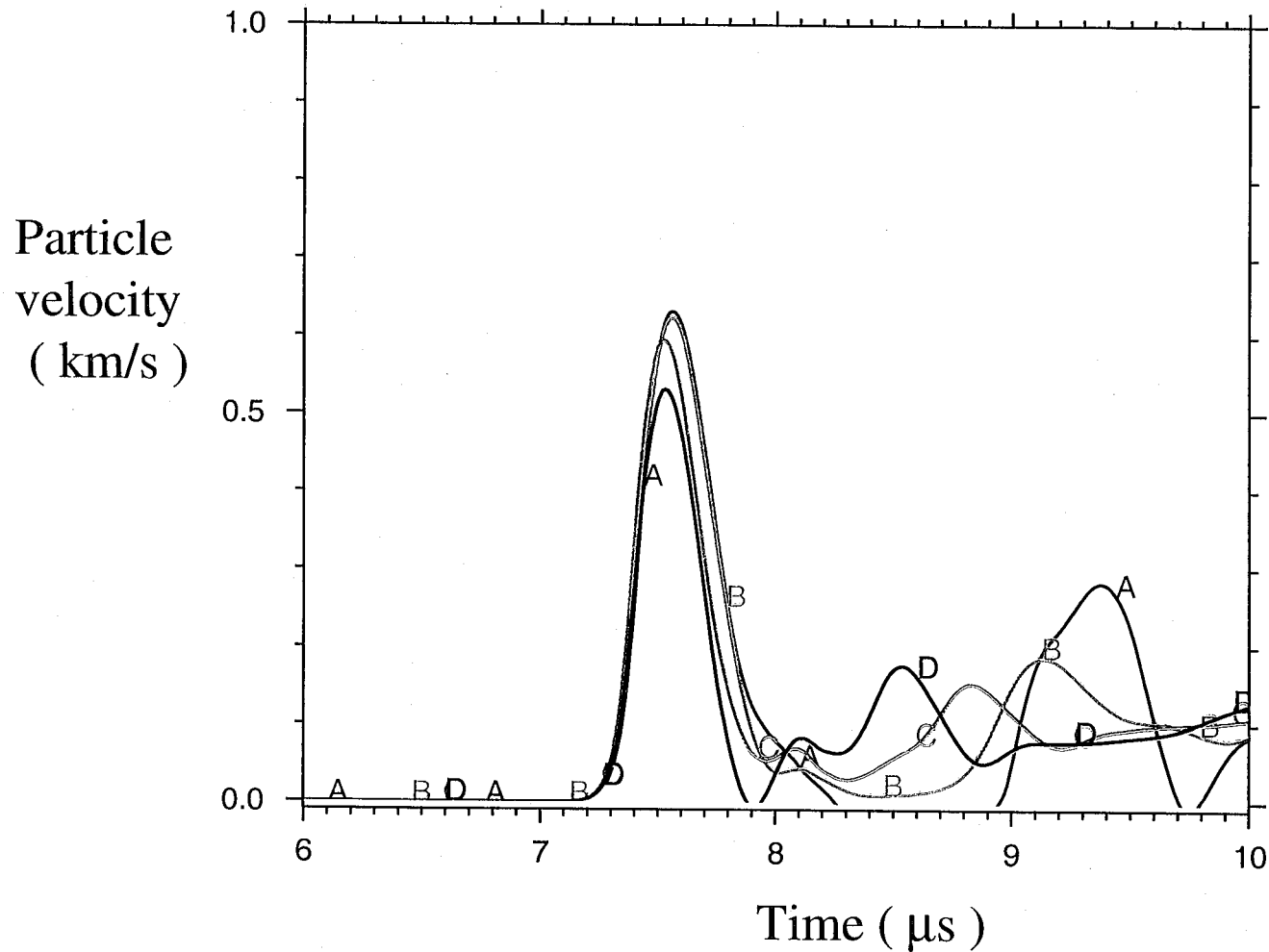


Figure 38

Second series NMD EOS experiments modeling calculations: little particle velocity profile dependence on zoning



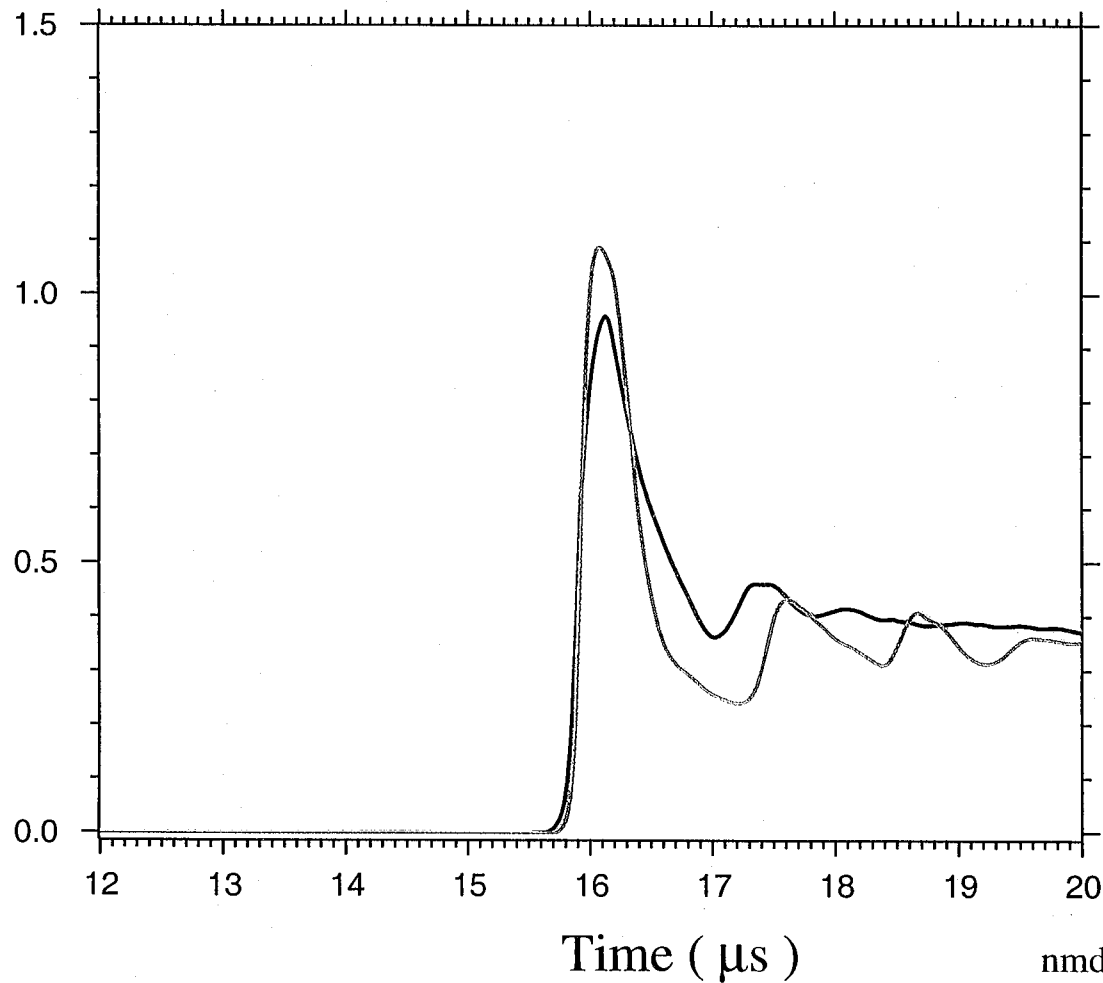
17mm dia. projectile 6km/s particle velocity at rear of witness plate on axis

Red: 150x113 zones

Blue: 240x225 zones

43

Particle
velocity
(km/s)



Time (μs)

nmda--38-mg-7-2-2001

Figure 39

Second series NMD EOS experiments modeling calculations: little particle velocity profile dependence on zoning



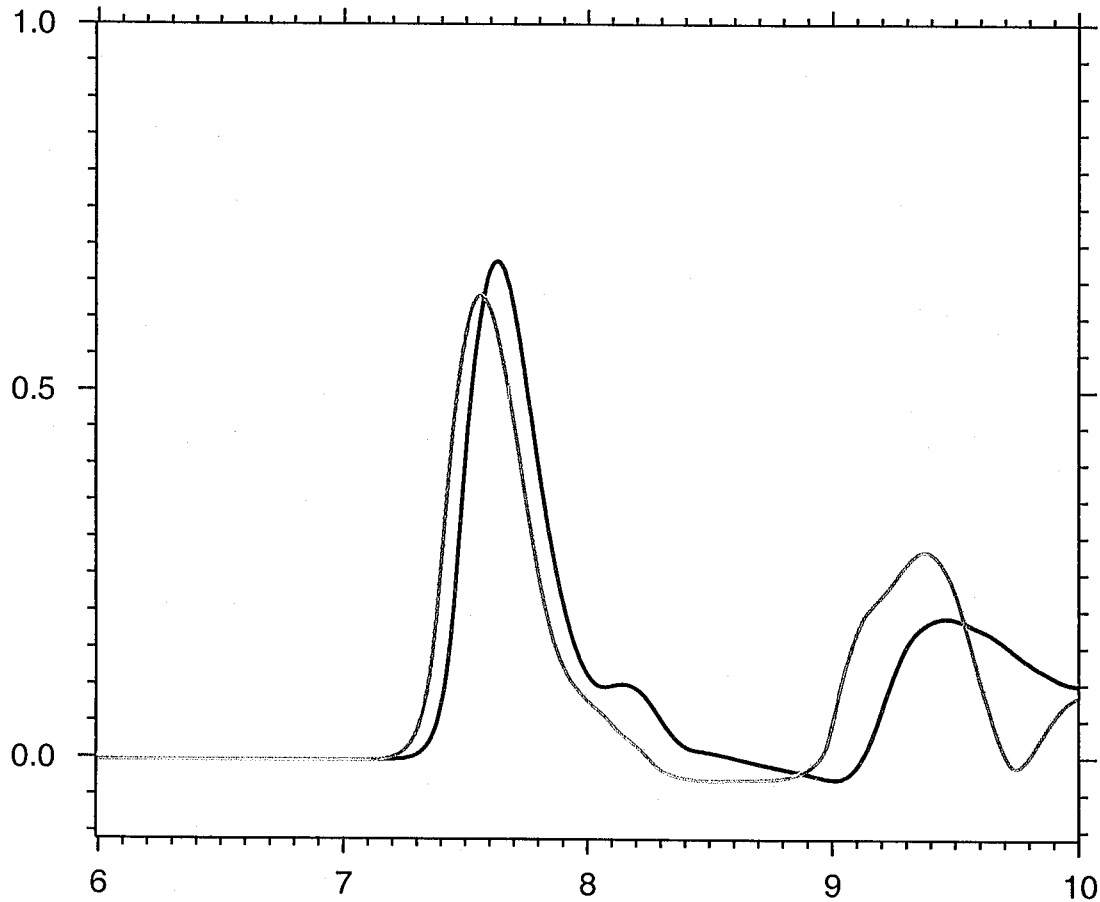
17mm dia. projectile 11km/s particle velocity at rear of witness plate on axis

Red: 150x113 zones

Blue: 240x225 zones

44

Particle
velocity
(km/s)



Time (μs)

nmda--39-mg-7-2-2001

Figure 40